EUR 3253.e

EUROPEAN ATOMIC ENERGY COMMUNITY - EURATOM
REACTOR CENTRUM NEDERLAND - RCN

JET PUMPS

by

J.T. WILMAN
(RCN)

1966

Contract No. 007-61-6 PNIN

This report is on sale at the addresses listed on cover page 4

at the price of FF 8.50	FB 85,—	DM 6.80	Lit. 1.060	Fl. 6.20

When ordening, please quote the EUR number and the title, which are indicated on the cover of each report.

Printed by Guyot, s.a.
Brussels, December 1966

EUR 3253.e

EUROPEAN ATOMIC ENERGY COMMUNITY - EURATOM
REACTOR CENTRUM NEDERLAND - RCN

JET PUMPS

by

J.T. WILMAN
(RCN)

1966

Contract No. 007-61-6 PNIN

The present publication is one of a series giving more detailed information on special subjects covered under the NERO development programme carried out by the Reactor Centrum Nederland in association with Euratom (Contract No. 007-61-6 PNIN).

A general description of the design data and the experimental work, which is aimed at the development of a pressurized-water reactor for marine application, is given in Euratom Reports:

"EUR 2180.e - NERO DEVELOPMENT PROGRAMME
Report covering the period January 1963 through June 1964"

"EUR 3125.e - NERO DEVELOPMENT PROGRAMME
Report covering the period of July 1964 to December 1965"

in which are listed also further publications in the above-mentioned series.

F O R E W O R D

Jet pumps are basically simple in construction and have no moving parts; in many cases they can be effectively used where the service conditions make it impractical to use mechanical pumps.

As it may also be advantageous to use jet pumps in nuclear reactor cooling systems with internal recirculation a study of jet pump behaviour was carried out under a research contract with the European Atomic Energy Community (Contract no 007-61-6 PNIN; NERO development programme, Reactor Centrum Nederland - Euratom).

The results of this study are presented in this report.

SUMMARY

In this report a *theoretical study* of the behaviour of jet pumps is made on the basis of a simplified model. Experiments carried out with the object of optimizing the performance of jet pumps are described. It is found that the theoretically predicted results are in good agreement with the experimental data for high performance jet pumps. Finally, it is shown how, for given conditions, absolute jet pump dimensions can be calculated.

JET PUMPS

CONTENTS

CONTENTS (continued)

J E T   P U M P S

A. INTRODUCTION (*)

An attempt was made to derive an equation by means of which the behaviour of jet pumps can be predicted.

To verify the theoretical results a low pressure, low temperature, experimental unit, having a jet pump as principal component, was designed and constructed. A test was performed at the Laboratory of Hydrodynamics at Delft Technological University.

With the object of optimizing jet pump performance the effects of internal changes to the experimental jet pump were also determined.

B. THE JET PUMP

A jet pump (figure 1) is a device in which a fluid flows through a driving nozzle which converts the fluid pressure into a high-velocity jet stream; fluid is continuously entrained from the suction section of the jet pump by the jet stream emerging from the nozzle. In the mixing tube the entrained fluid acquires part of the energy of the motive fluid. In the diffuser the velocity of the mixture is reconverted to pressure.

(*) Manuscript received on November 10, 1966

C. DERIVATION OF THE EQUATION REPRESENTING THE RELATIONSHIP BETWEEN THE TOTAL PRESSURE RATIO AND THE MASS FLOW RATIO

A generalized representation of a jet pump is shown in figure 1.

In this figure the planes A, B, W, Z and C are perpendicular to the axis of the jet pump;

A is a plane just upstream from the driving nozzle,

B is a plane in the suction section of the jet pump,

W is a plane just downstream from the nozzle discharge tip,

Z is a plane at the inlet end of the diffuser,

C is a plane at the outlet end of the diffuser.

If it is assumed that in a steady state the static pressure has the same value at all points in the plane W, then (Bernoulli's equation)

$$p_A - p_W = -\rho g(h_A - h_W) - \tfrac{1}{2}\rho(v_A^2 - v_s^2) + K_s.\tfrac{1}{2}\rho v_s^2 \ ,$$

$$p_B - p_W = -\rho g(h_B - h_W) - \tfrac{1}{2}\rho(v_B^2 - v_t^2) + K_t.\tfrac{1}{2}\rho v_t^2 \ ,$$

where

p_A is the static pressure in the plane A,

p_B is the static pressure in the plane B,

p_W is the static pressure in the plane W,

ρ is the density of the fluid,

g is the acceleration due to gravity,

h_A is the height of A above a reference level O-O,

h_B is the height of B above the reference level O-O,

h_W is the height of W above the reference level O-O,

v_A is the velocity of the motive fluid in the plane A,

v_B is the fluid velocity in the plane B,

v_s is the fluid velocity in the nozzle discharge tip,

v_t is the velocity of the entrained fluid in the plane W (suction annulus),

K_s is a loss coefficient which applies to the flow between the planes A and W,

K_t is a loss coefficient which applies to the flow between the planes B and W.

The assumption is made that in the plane W just downstream from the nozzle tip the total effective flow area is equal to the cross-sectional area of the mixing tube.

As the jet stream and the suction stream mix between the plane W and the plane Z at the outlet end of the mixing tube (figure 1), it follows from a consideration of the change in momentum between the planes W and Z that in a steady state, to a good approximation,

$$(G_1 + G_2)v_Z - G_1 v_s - G_2 v_t =$$

$$= (p_W - p_Z)S_m + \rho(h_W - h_Z)S_m g - K_m \cdot \tfrac{1}{2}\rho v_Z^2 S_m \ ,$$

where

G_1 is the mass flow rate in the driving nozzle,

G_2 is the mass flow rate in the suction section of the jet pump,

p_Z is the static pressure in the plane Z,

h_Z is the height of Z above the reference level 0-0,

v_Z is the fluid velocity in the plane Z,

S_m is the cross-sectional area of the mixing tube,

K_m is a loss coefficient which applies to the flow between the planes W and Z.

Therefore

$$p_W - p_Z = -\rho g(h_W - h_Z) + \frac{G_1 + G_2}{S_m} v_Z +$$

$$- \frac{G_1}{S_m} v_s - \frac{G_2}{S_m} v_t + K_m.\tfrac{1}{2}\rho v_Z^2 .$$

For the diffuser (Bernoulli's equation)

$$p_Z - p_C = -\rho g(h_Z - h_C) - \tfrac{1}{2}\rho(v_Z^2 - v_C^2) + K_d.\tfrac{1}{2}\rho v_Z^2 ,$$

where

p_C is the static pressure in the plane C,

h_C is the height of C above the reference level O-O,

v_C is the fluid velocity in the plane C,

K_d is a loss coefficient which applies to the flow between the planes Z and C.

As

$$p_B - p_C = (p_B - p_W) + (p_W - p_Z) + (p_Z - p_C) ,$$

it can be readily found that

$$p_B - p_C = -\rho g(h_B - h_C) - \tfrac{1}{2}\rho(v_B^2 - v_C^2) + \tfrac{1}{2}\rho(v_t^2 - v_Z^2) +$$

$$+ \frac{G_1 + G_2}{S_m} v_Z - \frac{G_1}{S_m} v_s - \frac{G_2}{S_m} v_t +$$

$$+ K_t.\tfrac{1}{2}\rho v_t^2 + K_m.\tfrac{1}{2}\rho v_Z^2 + K_d.\tfrac{1}{2}\rho v_Z^2 .$$

If H_B is the total pressure at B and H_C is the total pressure at C, then

$$H_B = p_B + \rho g h_B + \tfrac{1}{2}\rho v_B^2 \ ,$$

$$H_C = p_C + \rho g h_C + \tfrac{1}{2}\rho v_C^2 \ .$$

Hence

$$H_B - H_C = \frac{G_1 + G_2}{S_m} v_Z - \frac{G_1}{S_m} v_s - \frac{G_2}{S_m} v_t + $$

$$+ \tfrac{1}{2}\rho(1 + K_t)v_t^2 + \tfrac{1}{2}\rho(K_m + K_d - 1)v_Z^2 \ .$$

As it was assumed that the total effective area in the plane W is equal to S_m, the mass flow rate G_2 may be written as

$$G_2 = \rho v_t(S_m - S_s) \ ,$$

where S_s is the area of the nozzle discharge tip.

Since

$$G_1 = \rho v_s S_s \qquad \text{and} \qquad G_1 + G_2 = \rho v_Z S_m \ ,$$

it follows that

$$H_B - H_C = \rho v_Z^2 - \frac{S_s}{S_m}\rho v_s^2 - \frac{S_m - S_s}{S_m}\rho v_t^2 + $$

$$+ \tfrac{1}{2}\rho(1 + K_t)v_t^2 + \tfrac{1}{2}\rho(K_m + K_d - 1)v_Z^2 \ .$$

Consequently

$$H_C - H_B = \tfrac{1}{2}\rho v_s^2 \left\{ 2\frac{S_s}{S_m} + 2\frac{S_m - S_s}{S_m}\left(\frac{v_t}{v_s}\right)^2 + \right.$$

$$\left. - (1 + K_t)\left(\frac{v_t}{v_s}\right)^2 - (1 + K_m + K_d)\left(\frac{v_z}{v_s}\right)^2 \right\} .$$

If the mixing tube is cylindrical and the driving nozzle is cylindrical or conical, then a significant jet pump proportion is the diameter ratio δ, which is defined by

$$\delta = \frac{d_s}{d_m} \quad ,$$

where

d_s is the diameter of the nozzle discharge tip,

d_m is the diameter of the mixing tube.

Then

$$\frac{S_s}{S_m} = \frac{\frac{\pi}{4}\, d_s^2}{\frac{\pi}{4}\, d_m^2} = \left(\frac{d_s}{d_m}\right)^2 = \delta^2 \quad ,$$

$$\frac{S_m - S_s}{S_m} = 1 - \frac{S_s}{S_m} = 1 - \delta^2 \; .$$

If the mass flow ratio μ is defined by

$$\mu = \frac{G_2}{G_1} \quad ,$$

it follows that

$$\frac{v_t}{v_s} = \frac{G_2}{G_1}\,\frac{S_s}{S_m - S_s} = \mu\,\frac{\delta^2}{1-\delta^2} \quad ,$$

$$\frac{v_Z}{v_s} = \frac{G_1 + G_2}{G_1}\,\frac{S_s}{S_m} = (1+\mu)\,\delta^2 \quad .$$

Upon inserting the expressions for

$$\frac{S_s}{S_m} \quad , \quad \frac{S_m - S_s}{S_m} \quad , \quad \frac{v_t}{v_s} \quad \text{and} \quad \frac{v_Z}{v_s} \quad ,$$

it is found that

$$H_C - H_B = \tfrac{1}{2}\rho v_s^2 \left\{ 2\delta^2 + 2\mu^2\,\frac{\delta^4}{1-\delta^2} - (1+K_t)\mu^2\,\frac{\delta^4}{(1-\delta^2)^2} + \right.$$

$$\left. - (1 + K_m + K_d)(1+\mu)^2\delta^4 \right\} \quad .$$

It was already seen that in a steady state

$$p_A - p_W = -\rho g(h_A - h_W) - \tfrac{1}{2}\rho(v_A^2 - v_s^2) + K_s \cdot \tfrac{1}{2}\rho v_s^2 \quad ,$$

$$p_B - p_W = -\rho g(h_B - h_W) - \tfrac{1}{2}\rho(v_B^2 - v_s^2) + K_t \cdot \tfrac{1}{2}\rho v_t^2 \quad .$$

Hence

$$(p_A + \rho g h_A + \tfrac{1}{2}\rho v_A^2) - (p_B + \rho g h_B + \tfrac{1}{2}\rho v_B^2) =$$

$$= \tfrac{1}{2}\rho v_s^2 - \tfrac{1}{2}\rho v_t^2 + K_s . \tfrac{1}{2}\rho v_s^2 - K_t . \tfrac{1}{2}\rho v_t^2$$

or

$$H_A - H_B = \tfrac{1}{2}\rho v_s^2 \left\{ (1 + K_s) - (1 + K_t) \left(\frac{v_t}{v_s} \right)^2 \right\},$$

where H_A is the total pressure at A.

Consequently, since $\dfrac{v_t}{v_s} = \mu \dfrac{\delta^2}{1 - \delta^2}$,

$$H_A - H_B = \tfrac{1}{2}\rho v_s^2 \left\{ (1+K_s) - (1+K_t)\, \mu^2 \frac{\delta^4}{(1-\delta^2)^2} \right\}.$$

The total pressure ratio π is defined by

$$\pi = \frac{H_A - H_B}{H_C - H_B} .$$

Upon substituting the derived expressions for $H_C - H_B$ and $H_A - H_B$, it is found that

$$\pi = \frac{(1+K_s) - (1+K_t)\, \mu^2 \dfrac{\delta^4}{(1-\delta^2)^2}}{2\delta^2 + 2\mu^2 \dfrac{\delta^4}{1-\delta^2} - (1+K_t)\, \mu^2 \dfrac{\delta^4}{(1-\delta^2)^2} - (1+K_m+K_d)(1+\mu)^2 \delta^4}$$

D. THE THEORETICAL JET PUMP CHARACTERISTIC

By means of the derived expression for π the steady-state relationship between π and μ can be determined for specified values of δ, if the values of the loss coefficients K_s, K_t, K_m and K_d are known; the curve showing this theoretically found relationship (μ as a function of π) for a given diameter ratio δ may be called the theoretical jet pump characteristic.

As δ represents a relative proportion of jet pump parts the curve is valid for geometrically similar jet pumps, regardless of absolute dimensions.

It is evident that for a given value of δ the shape of the curve is dependent upon the values of the loss coefficients K_s, K_t, K_m and K_d; the values of π calculated for given values of μ are smaller for smaller values of the loss coefficients.

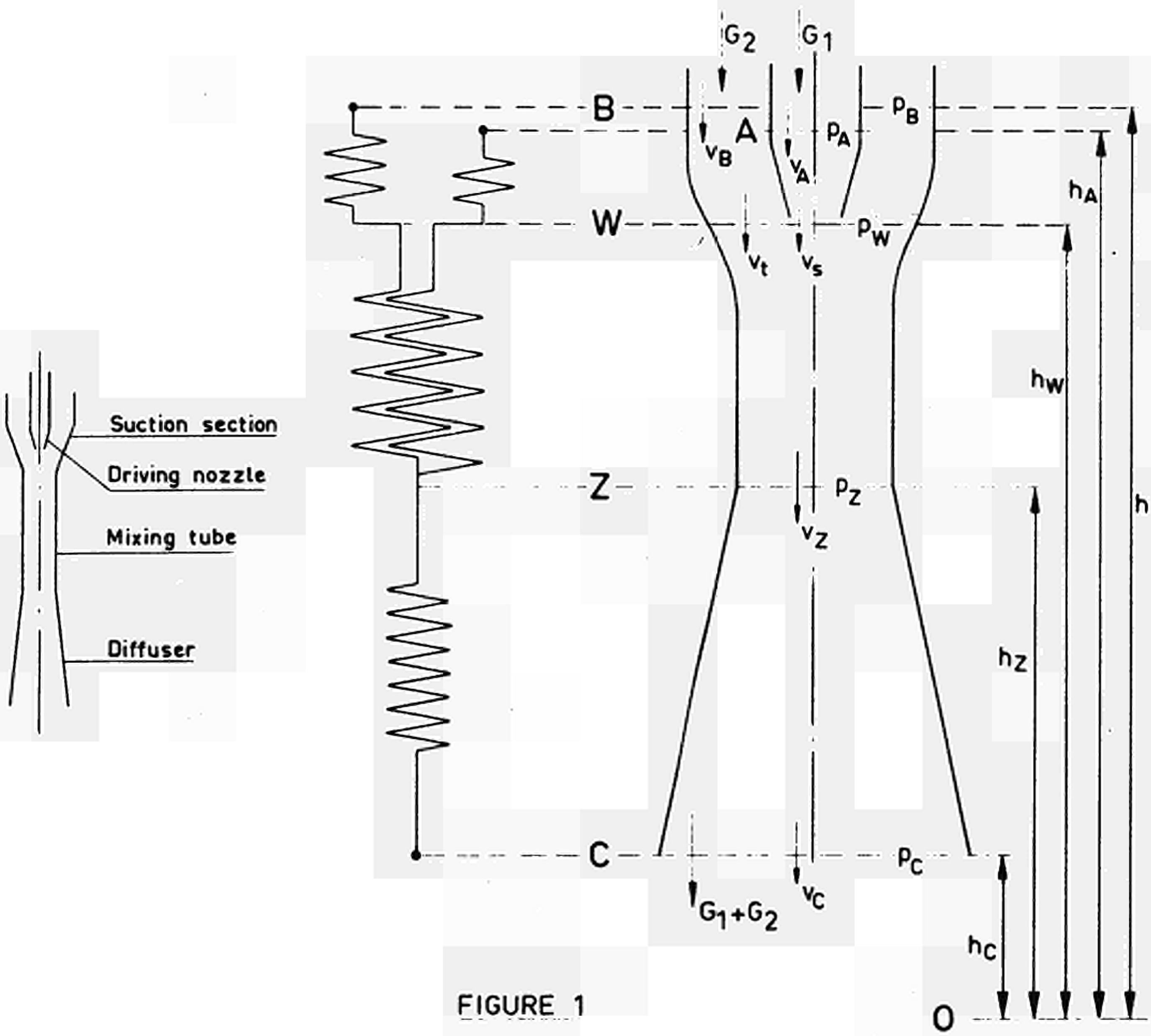

FIGURE 1

E. THE EFFICIENCY OF A JET PUMP

The efficiency η of a jet pump is defined by

$$\eta = \frac{Q_2(H_C - H_B)}{Q_1(H_A - H_C)} \quad ,$$

where

$$Q_1 = \frac{G_1}{\rho} \qquad \text{and} \qquad Q_2 = \frac{G_2}{\rho} \quad .$$

Hence,

$$\eta = \frac{G_2}{G_1} \frac{H_C - H_B}{(H_A - H_B) - (H_C - H_B)} = \frac{G_2}{G_1} \frac{1}{\dfrac{H_A - H_B}{H_C - H_B} - 1} =$$

$$= \frac{\mu}{\pi - 1} \quad .$$

The maximum jet pump efficiency is determined by the maximum value of $\frac{\mu}{\pi - 1}$.

If a line through a point (π_1, μ_1) of a jet pump characteristic and the point (1,0) on the π-axis (figure 2) makes an angle γ with the π-axis, then

$$\tan \gamma = \frac{\mu_1}{\pi_1 - 1} = \eta_1 \quad ,$$

where η_1 is the jet pump efficiency for the point (π_1, μ_1) of the characteristic.

It can be seen from figure 2 that the line intersects the jet pump characteristic at two points; this means that there are two different values of the mass flow ratio (μ_1 and μ_2) for the same jet pump efficiency.

The angle between the π-axis and the line through the point (1, 0) is a maximum (γ_m) if the line is a tangent to the characteristic; therefore, the point of contact (π_m, μ_m) is the point of maximum jet pump efficiency.

Consequently, if η_m is the maximum efficiency,

$$\eta_m = \frac{\mu_m}{\pi_m - 1} \quad .$$

It is evident that the performance of a jet pump is dependent upon the shape of the jet pump characteristic.

As the theoretical characteristic for a given value of the diameter ratio δ is determined by the values of the loss coefficients K_s, K_t, K_m and K_d it is to be expected that the performance of a jet pump will be dependent upon the shape of the fluid passages, the degree of roughness of the internal surfaces, the velocities in the fluid passages, the density and the viscosity of the fluid, etc.

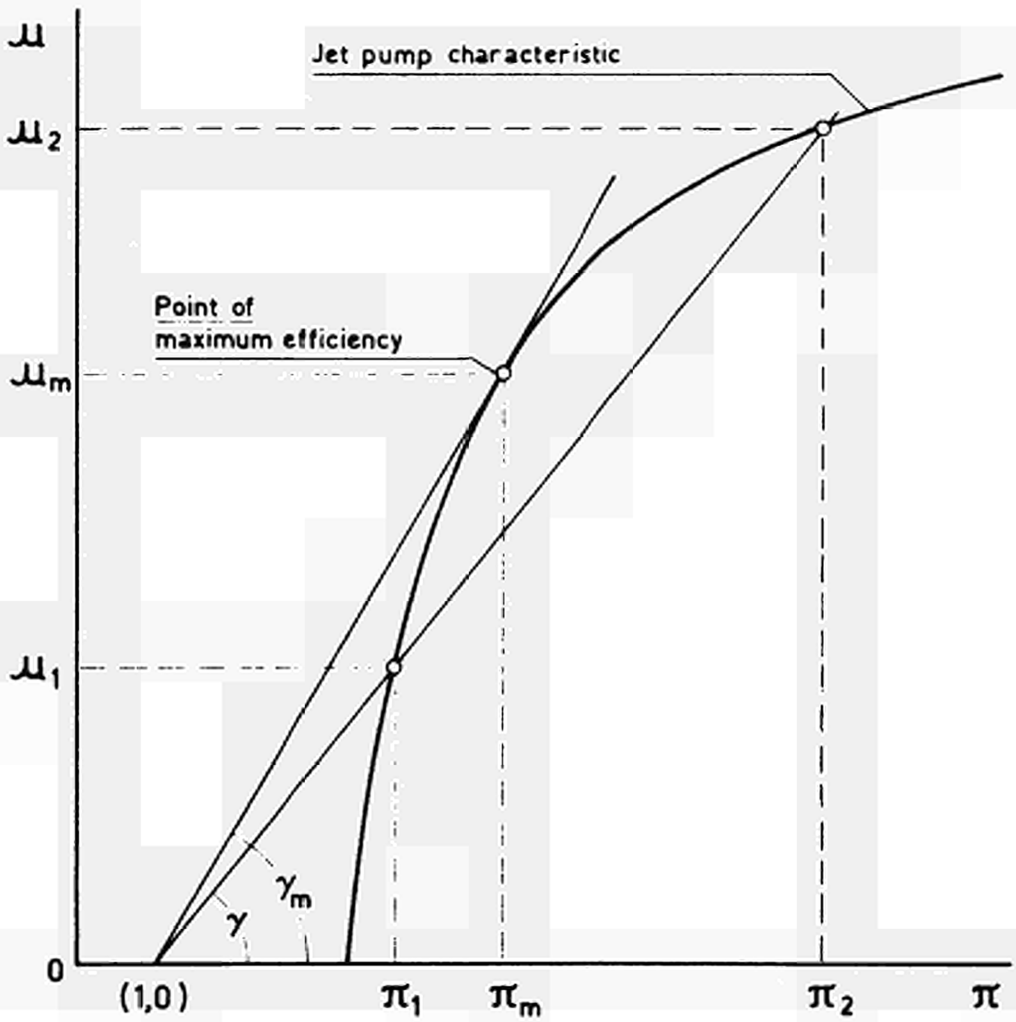

FIGURE 2

. THE EXPERIMENTAL EQUIPMENT

The experimental unit is schematically represented in figure 3; the principal components were a jet pump, a tank, a motor-driven centrifugal pump and a U-tube manometer board.

The jet pump mainly consisted of a conical driving nozzle, a cylindrical mixing tube and a cone-shaped diffuser (figure 1).

Water was the fluid used in the experimental unit; the centrifugal pump had a capacity of 0.013 m^3/sec at a total head of approximately 50 m. The pump motor required a 380-volt, 3-phase, 50-cycle power supply.

A diagram of the flow system is shown in figure 4.

The system is characterized by the positions

A just upstream from the driving nozzle,

B in the suction section of the jet pump,

C at the diffuser outlet,

D in the tank,

E in the suction nozzle of the centrifugal pump,

F in the discharge nozzle of the centrifugal pump.

It is seen from figure 4 that the system consists of a pump circuit F A C D E F (mass flow rate G_1) and a jet pump circuit C D B C (mass flow rate G_2); these circuits are coupled by the jet pump.

Flow rates could be controlled by valves in the pump discharge and bypass lines, in the jet pump suction line and in the jet pump discharge line (figure 3).

The flow rates could be determined by means of an orifice plate O_1 in the pump discharge line and an orifice plate O_2 in the jet pump discharge line.

To measure the pressure drops across the orifice plates U-tube manometers were used.

The experimental unit permitted constant temperature operation; it was possible to increase the temperature by means of electric heating elements. The maximum operating temperature was about 65°C.

Static pressure taps were located in three rows along the length of the jet pump; there were three pressure taps in each of the planes B, W, R, T, X, Y, Z and C perpendicular to the axis of the jet pump (figures 3 and 5).

Differential pressures between these static taps and a static tap at the position D in the tank could be determined with a set of U-tube manometers containing mercury (Hg) as an indicating fluid (figure 3).

Static pressures at D and in the plane A just upstream from the driving nozzle could be measured by means of the spring-type gauges M_D and M_A, respectively (figures 3 and 5).

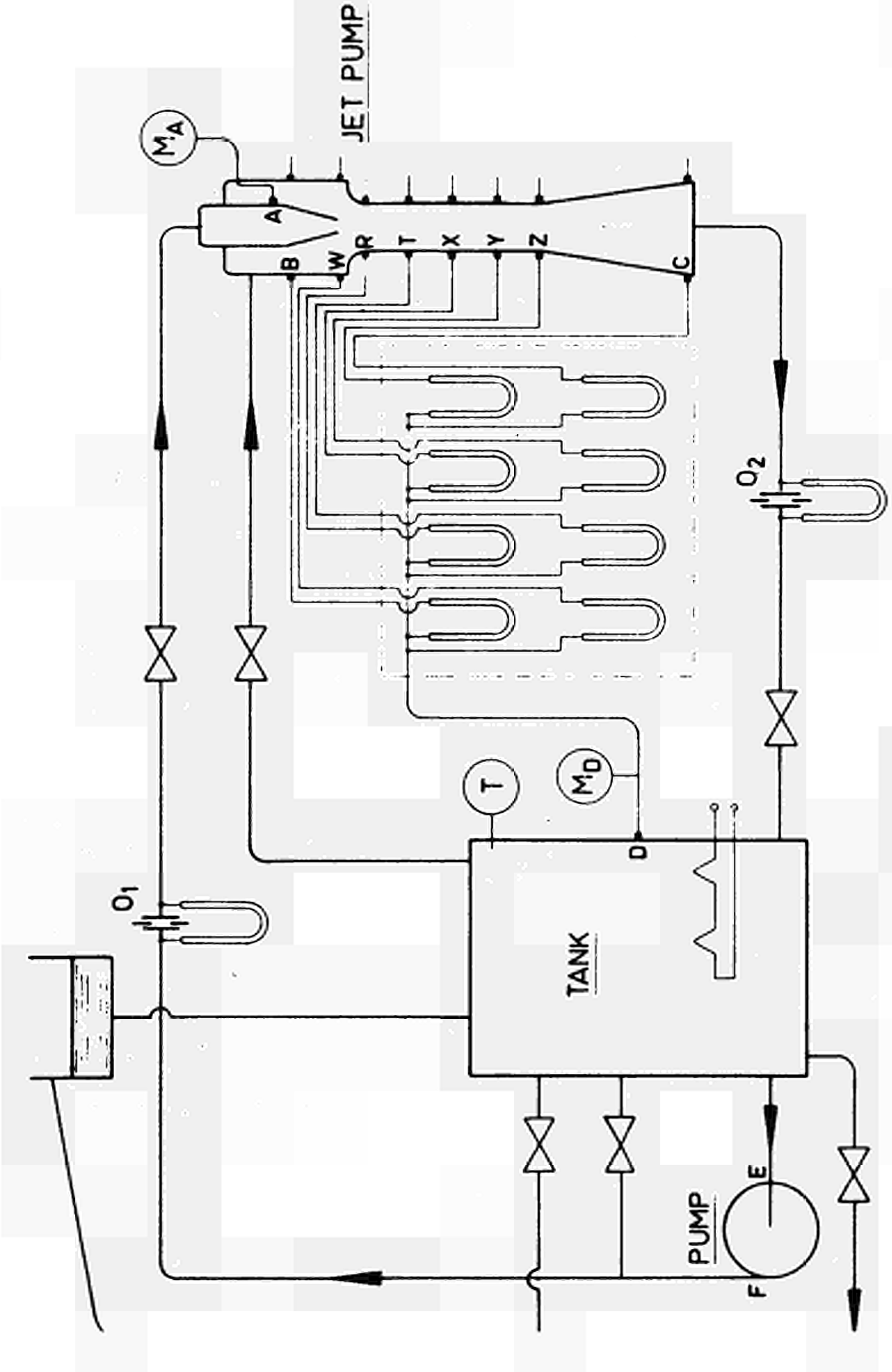

FIGURE 3

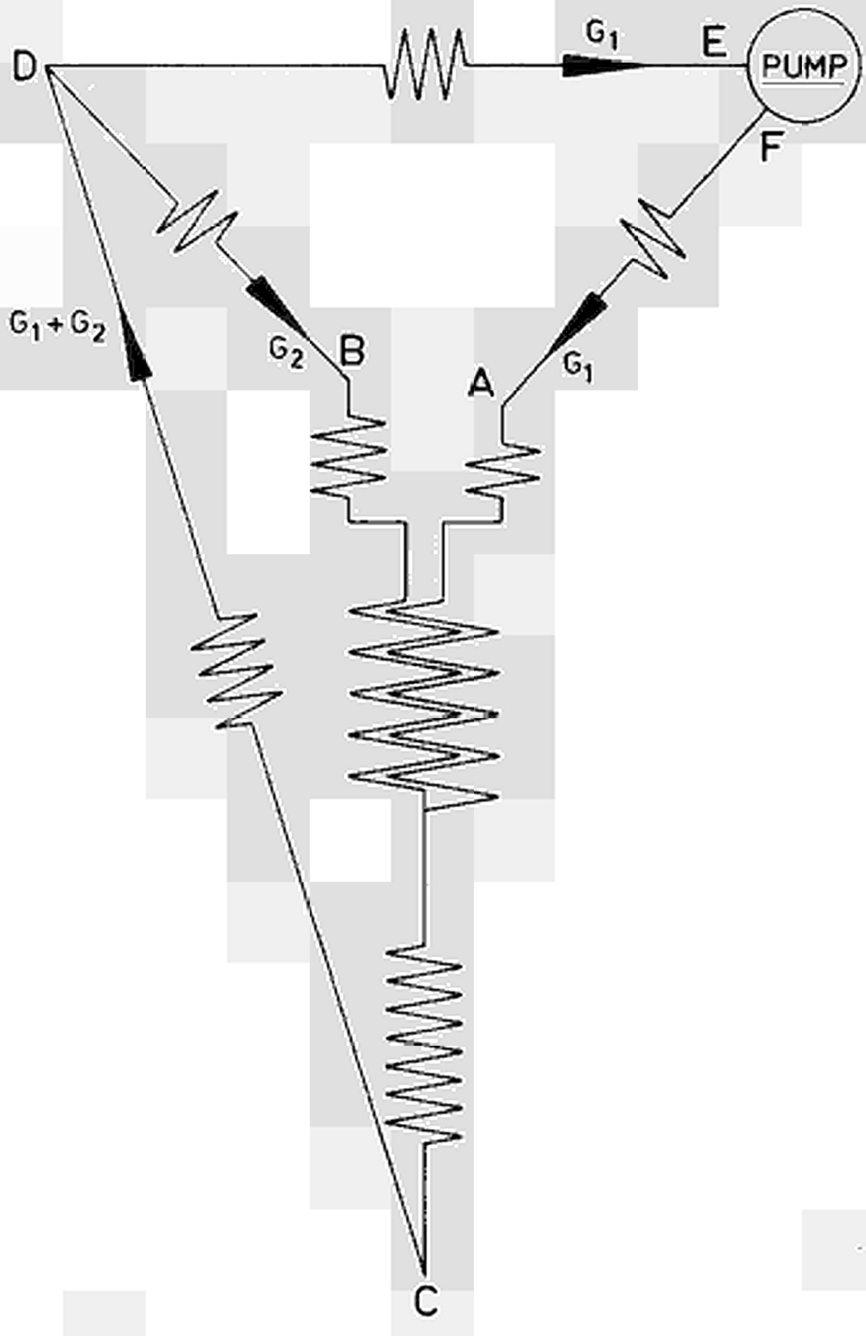

FIGURE 4

G. THE TEST

The experimental equipment was found to operate satisfactorily.

The test was performed in 13 phases. In each phase many test runs were made at different conditions.

Flow rates (fluid velocities) were easily controlled over the entire range of operation by means of the control valves in the system.

Readings of all U-tube manometers and pressure gauges (figure 3) were taken during each test run.

Three different driving nozzles were used during the test; with these nozzles the values of the diameter ratio δ of the jet pump were 0.439, 0.403 and 0.339, respectively.

During phase I only preliminary measurements were made; the internal surfaces of the jet pump were relatively rough (galvanized).

After phase I the internal surfaces of the jet pump components were normally polished.

During the phases II and III the driving nozzle was supported in the suction section of the jet pump (down-stream from the plane B; figures 1 and 5) by three radial plates parallel to the flow. These supporting plates were removed after phase III.

After phase VI the radius r of the rounding of the mixing tube entrance (figure 5) was changed from $r = 5\ d_m$ to $r = 0.5\ d_m$.

In phase IX the fluid temperature (t) was maintained at 57°C; during all other phases the temperature was 25°C.

It was possible to vary the eccentricity of the jet pump driving nozzle. Test runs were made at three different values of the eccentricity ratio e, which is defined by

$$e = 2 \times \frac{\text{radial displacement from the concentric position}}{d_m - d_s}.$$

The distance l_e between the nozzle discharge tip and the beginning of the mixing tube (figure 5) could also be varied. In phase XII the distance l_e was equal to $0.4\ d_m$; in all other phases the distance l_e was about $0.7\ d_m$.

As the performance of the driving nozzle and the efficiency of the diffuser were found to be excellent no further investigations were made into the effect of design changes to the nozzle and the diffuser.

The conditions during each phase of the test are summarized in table 1.

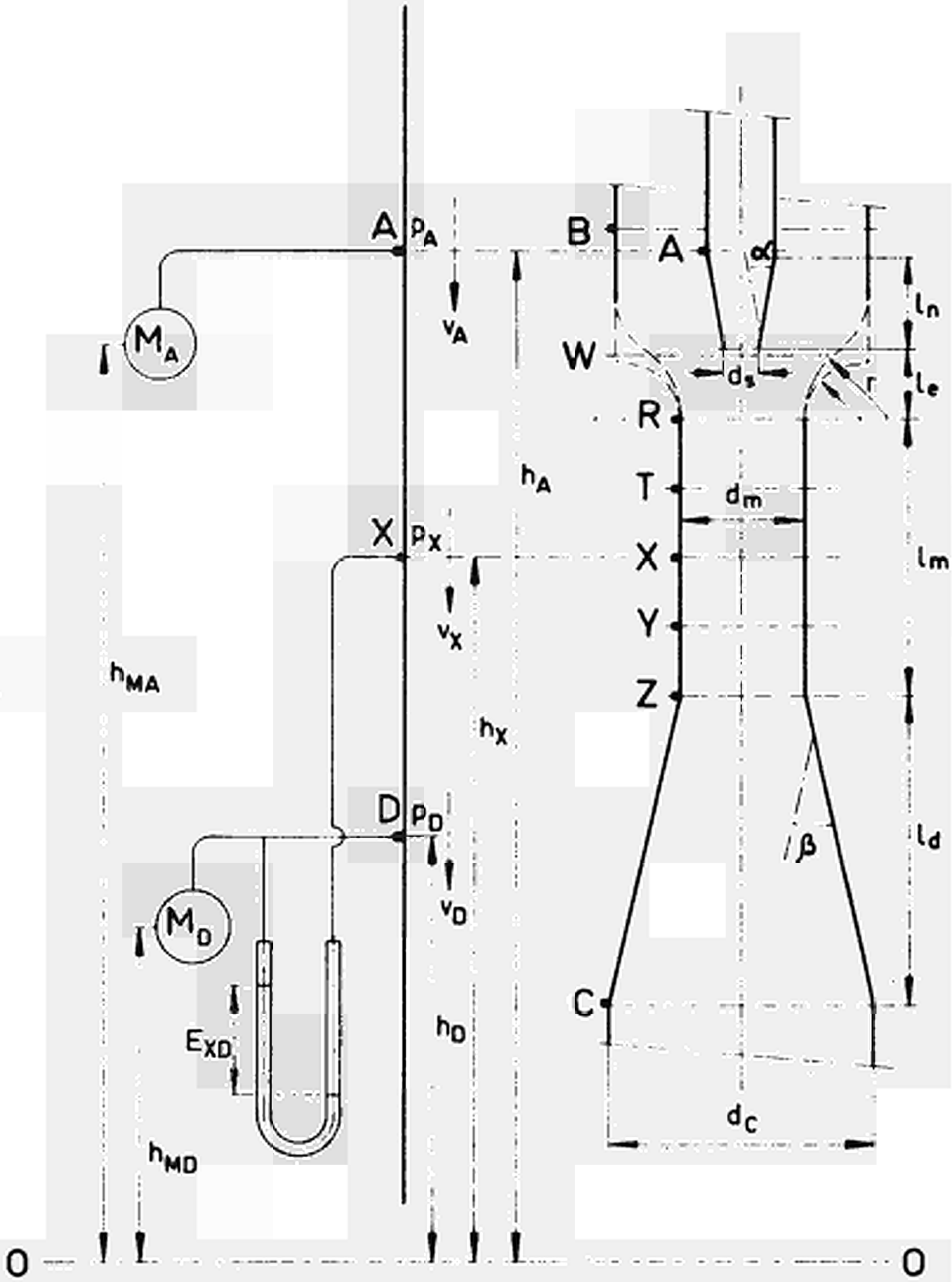

A
p_A
v_A
M_A
X
p_X
v_X
h_A
h_{MA}
h_X
D
p_D
v_D
M_D
E_{XD}
h_D
h_{MD}
O
O
B
A
W
R
T
X
Y
Z
C
α
d_s
r
l_n
l_e
d_m
l_m
β
l_d
d_C

FIGURE 5

H. TEST RESULTS

Test results are given in the tables 2, 3, 4, 5, 6, 7, 8, 9, 10, 11, 12 and 13 (Appendix). The tabulated values of $E_A - E_D$, v_s, μ and π were calculated from the test readings by means of the expressions derived in the Appendix ("Reduction of the test data").

The values of μ and π were used in determining jet pump characteristic curves; in the figures 6, 7, 8, 10, 11, 13 and 16 these experimentally determined curves are shown.

The jet pump had a conical driving nozzle with smooth internal and external surfaces. The length l_n of the conical part of the nozzle (figure 5) was equal to about 6 times the diameter d_s of the discharge tip; the average convergence angle α was 13^o. As this type of nozzle showed excellent discharging properties no other types were tested.

From figure 6 (phases II and IV) it is seen that thin plates supporting the nozzle may have a favourable effect on the shape of the jet pump characteristic. Apparently the supporting plates act as guide vanes.

Figure 7 (phases VI and VII) shows the effect of a change in the radius r of the rounding of the mixing tube entrance ($r = 5\ d_m$ and $r = 0.5\ d_m$).

Effects of the velocity v_s in the nozzle discharge tip are shown in figure 10 and figure 11 (phases IV and VIII, respectively).

The results shown in figure 12 (phases VIII and IX) appear to indicate that the effect of temperature (density, viscosity) is negligible.

Jet pump characteristics ($\delta = 0.403$) for three different values of the eccentricity ratio e ($e = 0.16$, phase VII; $e = 0$, phase X and $e = 0.35$, phase XI) are shown in figure 8. It is seen from this figure that eccentricity of the nozzle does not exhibit a significant effect for small values of the eccentricity ratio (up to about $e = 0.16$).

High jet pump efficiency was obtained for $l_e = 0.7\ d_m$. From figure 13 (phases X and XIII) it can be easily determined that

$$\text{for } \delta = 0.403 \quad \text{the maximum efficiency is } \frac{1.36}{5.2 - 1} = 35.8,$$

$$\text{for } \delta = 0.339 \quad \text{the maximum efficiency is } \frac{2.53}{8.1 - 1} = 35.6,$$

The effect of small variations in the distance l_e (between the nozzle tip and the beginning of the mixing tube) appears to be negligible. From figure 9 (phases X and XII) it can be seen that for a diameter ratio δ equal to 0.403 even a decrease of l_e by about 40% (l_e from $0.7\ d_m$ to $0.4\ d_m$) does not affect the shape of the jet pump characteristic.

The length l_m of the mixing tube (figure 5) was 8 times the diameter d_m. During all test runs at high jet pump efficiency the static pressure exhibited a maximum near the outlet end of the mixing tube (figure 14); this means that with the chosen length complete mixing is attained. In a longer tube the static pressure will decrease again toward the outlet end due to frictional losses; this will result in a decrease in jet pump efficiency. It is evident, therefore, that for a jet pump of good performance the length l_m of the mixing tube is equal to about 8 d_m.

The length l_d of the cone-shaped diffuser (figure 5) was equal to about 10 d_m; the divergence angle β was 7°. During the first phases of the test it was found that the efficiency of the diffuser ranged from 0.80 to 0.90. As the efficiency of a good diffuser is about 0.85 no further investigations were made into the effect of design changes to the diffuser.

PHASE	δ			e			r		l_e		t		TABLE	FIGURE
	0.439	0.403	0.339	0.16	0	0.35	$5d_m$	$0.5d_m$	$0.7d_m$	$0.4d_m$	25°C	57°C		
I			○	○			○		○		○		—	—
II	○			○			○		○		○		2	6
III			○	○			○		○		○		3	—
IV	○			○			○		○		○		4	6,10
V			○	○			○		○		○		5	—
VI		○		○			○		○		○		6	7
VII		○		○				○	○		○		7	7,8
VIII	○			○				○	○		○		8	11,12
IX	○			○				○	○			○	9	12
X		○			○			○	○		○		10	8,9,13,16
XI		○				○		○	○		○		11	8
XII		○			○			○		○	○		12	9
XIII			○		○			○	○		○		13	13,16

All phases : $l_m = 8d_m$, $l_d = 10d_m$
Phases II and III : Supporting plates in suction section

Phase I : Internal surfaces relatively rough (galvanized)
Other phases : Internal surfaces smooth (normally polished)

TABLE 1

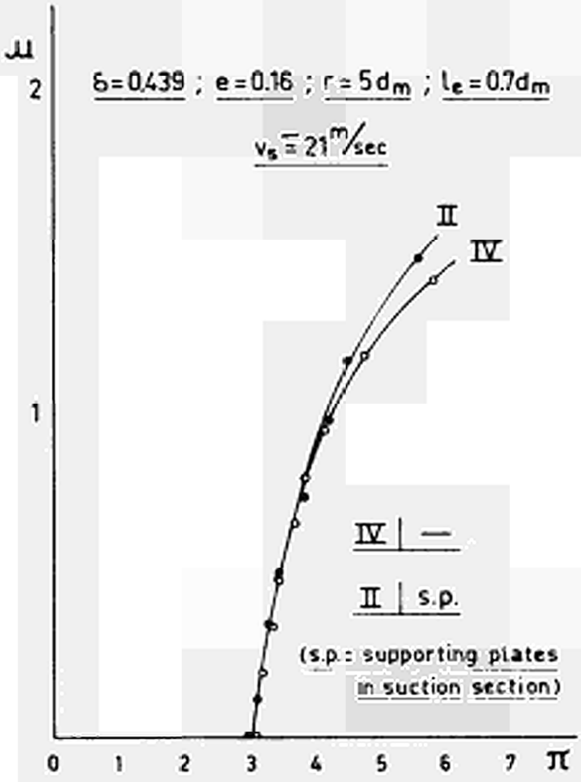

FIGURE 6

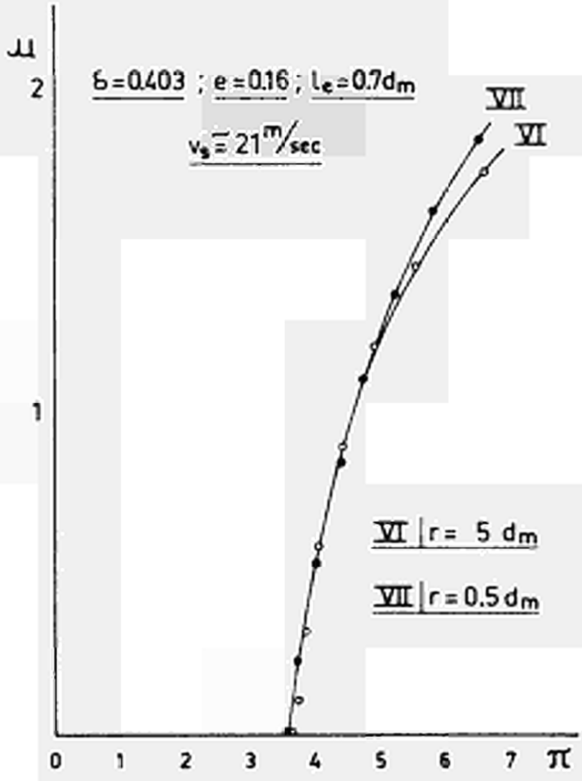

FIGURE 7

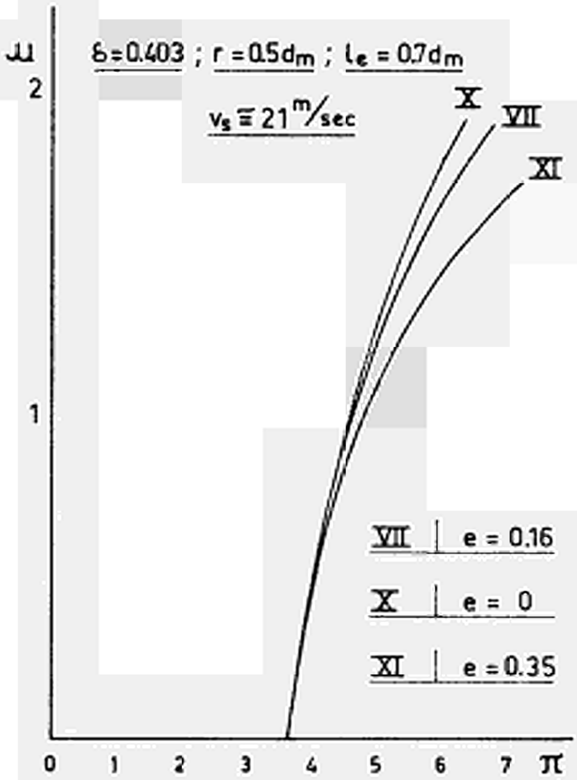

FIGURE 8

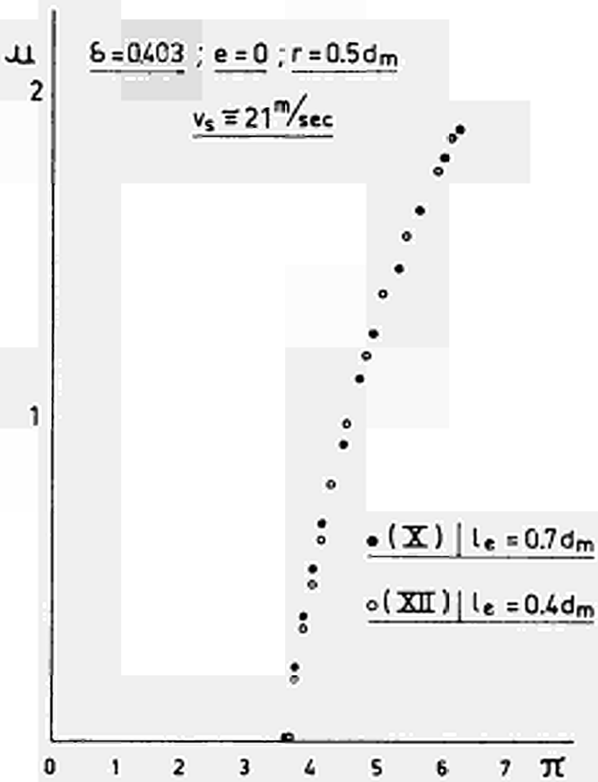

FIGURE 9

I. EVALUATION OF THE THEORETICAL LOSS COEFFICIENTS

I.1. Evaluation of K_m

It is a good idealization to assume that in the mixing tube the pressure loss Δp_m due to friction is

$$\Delta p_m = f_m \frac{L}{d_m} \cdot \tfrac{1}{2} \rho v_a^2 \quad ,$$

where

f_m is a friction factor,

L is the effective length of the mixing tube,

v_a is the average velocity along the wall of the mixing tube.

If, for simplicity, it is assumed that (figure 1)

$$v_a = \frac{v_Z + v_t}{2} \quad ,$$

it follows that

$$\Delta p_m = f_m \cdot \frac{L}{d_m} \left(\tfrac{1}{2} + \tfrac{1}{2} \frac{v_t}{v_Z} \right)^2 \cdot \tfrac{1}{2} \rho v_Z^2 \quad .$$

The pressure loss in the mixing tube was also written as

$$K_m \cdot \tfrac{1}{2} \rho v_Z^2 \quad .$$

Hence

$$K_m = f_m \cdot \frac{L}{d_m} \left(\tfrac{1}{2} + \tfrac{1}{2} \frac{v_t}{v_Z} \right)^2 \quad .$$

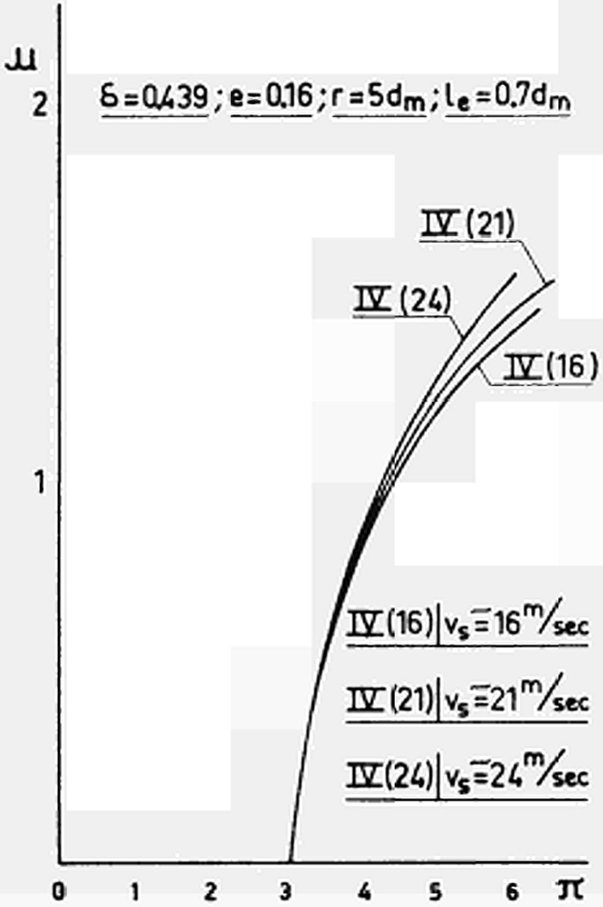

FIGURE 10

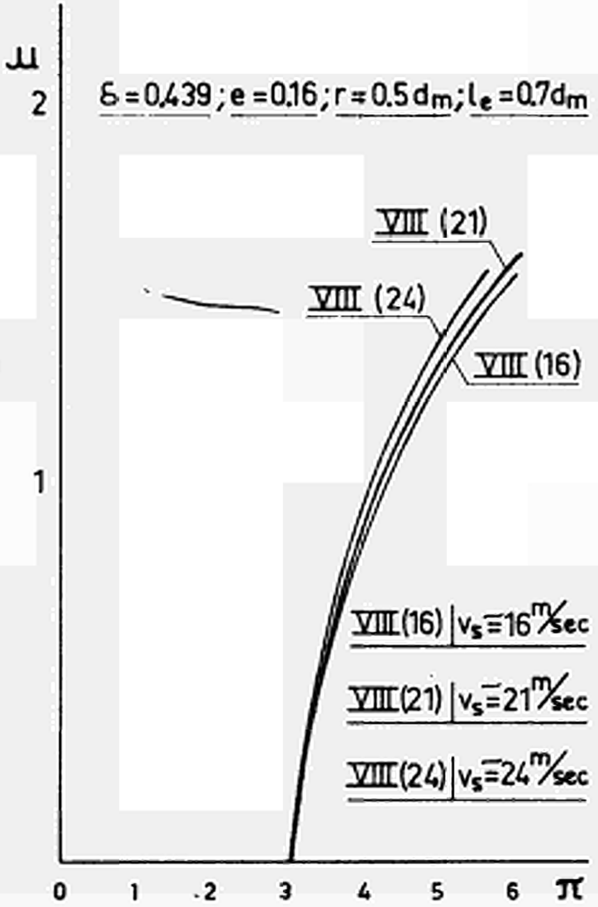

FIGURE 11

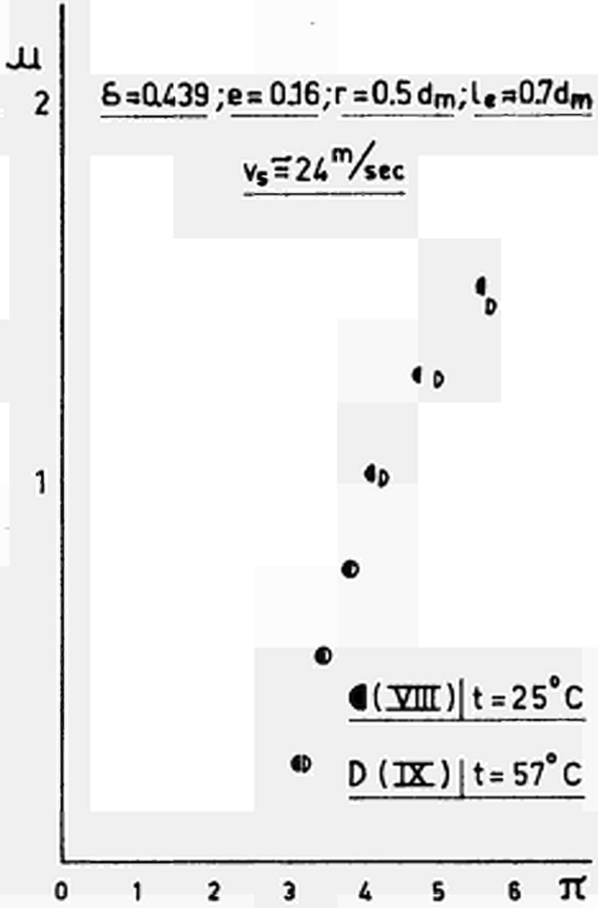

FIGURE 12

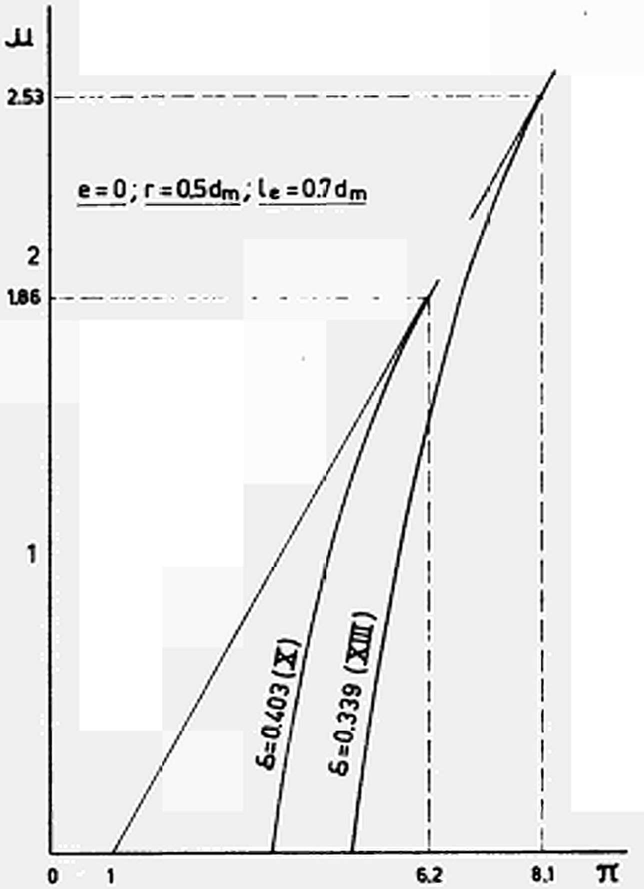

FIGURE 13

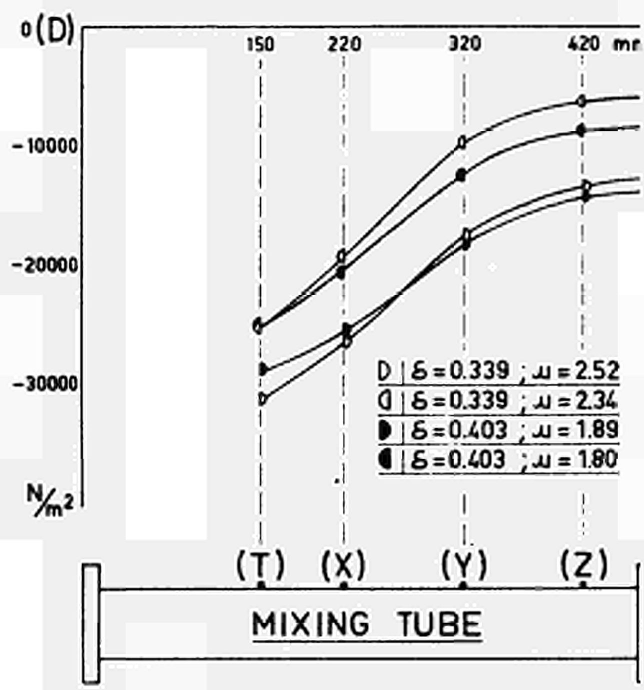

FIGURE 14

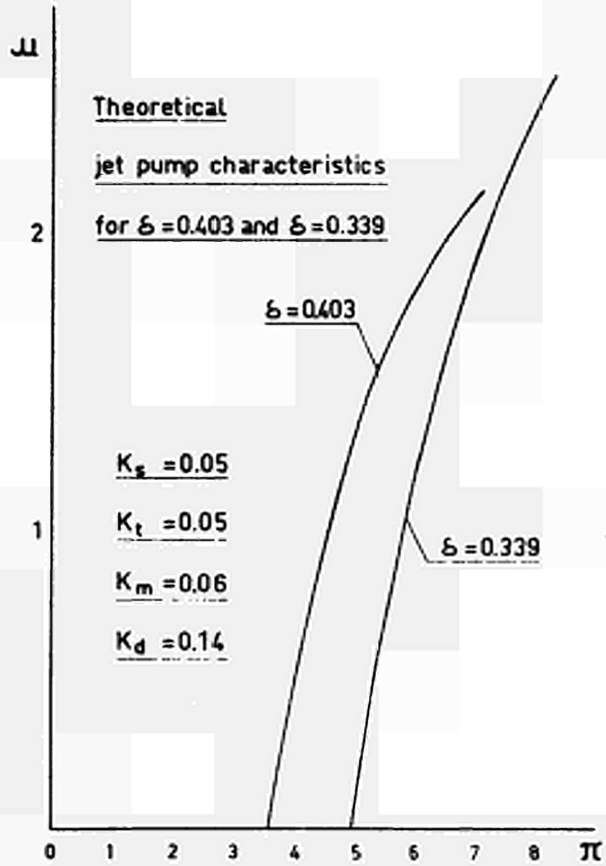

FIGURE 15

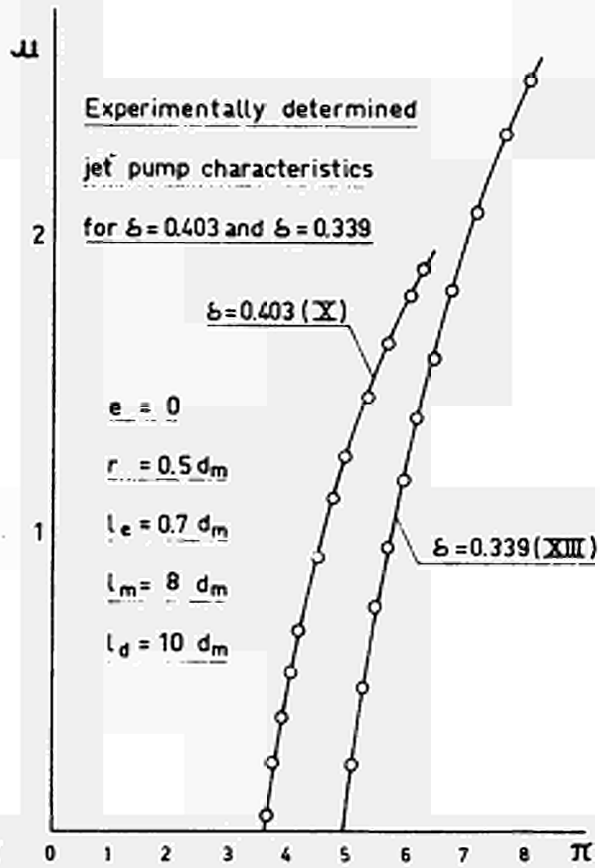

FIGURE 16

From

$$\rho v_s S_s + \rho v_t (S_m - S_s) = \rho v_Z S_m$$

it can be found that

$$v_s - v_t = \frac{S_m}{S_s} (v_Z - v_t) \quad .$$

Since $v_s - v_t > 0$, it follows that

$$v_Z - v_t > 0$$

or $$\frac{v_t}{v_Z} < 1 \quad .$$

A good approximation is obtained if it is assumed that

$$\frac{v_t}{v_Z} = 0.5 \qquad \text{and} \qquad L = 0.75\ l_m \quad .$$

Then

$$K_m = f_m \frac{0.75\ l_m}{d_m} (\tfrac{1}{2} + \tfrac{1}{2} \times 0.5)^2 \quad .$$

For a smooth internal surface of the mixing tube the value of the friction factor f_m may be taken as 0.018.

Consequently, if $\frac{l_m}{d_m} = 8$,

$$K_m = 0.018 \times 0.75 \times 8\ (\tfrac{1}{2} + \tfrac{1}{2} \times 0.5)^2 =$$
$$= 0.018 \times 0.75 \times 8 \times 0.75^2 = 0.06 \quad .$$

1.2. Evaluation of K_d

The efficiency η_d of the diffuser (figure 1) is defined by

$$\eta_d = \frac{(p_C + \rho g h_C) - (p_Z + \rho g h_Z)}{\frac{1}{2}\rho(v_Z^2 - v_C^2)} \quad .$$

Therefore

$$(p_C + \rho g h_C) - (p_Z + \rho g h_Z) = \eta_d \cdot \tfrac{1}{2}\rho(v_Z^2 - v_C^2) \quad .$$

It was already seen that for the diffuser

$$p_Z - p_C = -\rho g(h_Z - h_C) - \tfrac{1}{2}\rho(v_Z^2 - v_C^2) + K_d \cdot \tfrac{1}{2}\rho v_Z^2$$

or

$$(p_C + \rho g h_C) - (p_Z + \rho g h_Z) = \tfrac{1}{2}\rho(v_Z^2 - v_C^2) - K_d \cdot \tfrac{1}{2}\rho v_Z^2 \, .$$

Hence

$$\eta_d \cdot \tfrac{1}{2}\rho(v_Z^2 - v_C^2) = \tfrac{1}{2}\rho(v_Z^2 - v_C^2) - K_d \cdot \tfrac{1}{2}\rho v_Z^2$$

or

$$K_d = (1 - \eta_d)\left\{1 - \left(\frac{v_C}{v_Z}\right)^2\right\} \quad .$$

Since $\rho v_C S_C = \rho v_Z S_m$,

it follows that

$$\frac{v_C}{v_Z} = \frac{S_m}{S_C} = \left(\frac{d_m}{d_C}\right)^2 ,$$

where d_C is the diameter of the diffuser outlet (figure 5).

Therefore

$$K_d = (1 - \eta_d)\left\{1 - \left(\frac{d_m}{d_C}\right)^4\right\} \quad .$$

If the length l_d of the cone-shaped diffuser is equal to 10 d_m and the divergence angle β is 7^o (figure 5), then it can be readily found that

$$\begin{aligned} d_C &= d_m + 2\, l_d \tan \frac{\beta}{2} = \\ &= d_m + 20\, d_m \tan 3^o30' = \\ &= (1 + 20 \times 0.0612)\, d_m = \\ &= 2.22\, d_m \ . \end{aligned}$$

Hence

$$\frac{d_m}{d_C} = \frac{1}{2.22} \ .$$

The average value of the diffuser efficiency η_d was found to be about 0.85.

Consequently

$$\begin{aligned} K_d &= (1 - \eta_d) \left\{ 1 - \left(\frac{d_m}{d_C} \right)^4 \right\} = \\ &= (1 - 0.85) \left\{ 1 - \left(\frac{1}{2.22} \right)^4 \right\} = \\ &= 0.14 \ . \end{aligned}$$

I.3. Evaluation of K_s and K_t

From the derived expression for the total pressure ratio π it follows that the total pressure ratio for $\mu = 0$, represented by $(\pi)_{\mu=0}$, is given by

$$(\pi)_{\mu=0} = \frac{1 + K_s}{2\delta^2 - (1 + K_m + K_d)\delta^4} .$$

Hence

$$K_s = (\pi)_{\mu=0} \left\{ 2\delta^2 - (1 + K_m + K_d)\delta^4 \right\} - 1 .$$

As it was found that $K_m = 0.06$ and $K_d = 0.14$, it follows that

$$1 + K_m + K_d = 1.2$$

and

$$K_s = (\pi)_{\mu=0} \left(2\delta^2 - 1.2\delta^4 \right) - 1 .$$

The value of $(\pi)_{\mu=0}$ is represented by the point at which the jet pump characteristic curve intersects the π-axis (figure 2).

From the experimentally determined jet pump characteristics it is readily seen that

$(\pi)_{\mu=0} = 4.95$ for $\delta = 0.339$ (figures 13 and 16),

$(\pi)_{\mu=0} = 3.60$ for $\delta = 0.403$ (figures 7, 8, 13 and 16),

$(\pi)_{\mu=0} = 3.05$ for $\delta = 0.439$ (figures 6, 10 and 11).

From these conditions the average value for K_s is found to be about 0.05.
The loss coefficient K_t may be taken equal to K_s:

$$K_s = K_t = 0.05 .$$

J. CHARACTERISTICS AND MAXIMUM EFFICIENCY

Upon inserting the values

$$K_s = 0.05, \quad K_t = 0.05, \quad K_m = 0.06 \quad \text{and} \quad K_d = 0.14$$

into the derived expression for the total pressure ratio π, the result is

$$\pi = \frac{1.05 - 1.05\mu^2 \dfrac{\delta^4}{(1-\delta^2)^2}}{2\delta^2 + 2\mu^2 \dfrac{\delta^4}{1-\delta^2} - 1.05\mu^2 \dfrac{\delta^4}{(1-\delta^2)^2} - 1.2(1+\mu)^2\,\delta^4} .$$

By means of this expression theoretical characteristics (μ as a function of π) were determined for $\delta = 0.403$ and $\delta = 0.339$.
It can be seen from figure 15 and figure 16 that these characteristics agree excellently with the experimentally found characteristic curves for e = 0, r = 0,5 d_m, l_e = 0.7 d_m, l_m = 8 d_m and l_d = 10 d_m (phases X and XIII).
Theoretical characteristics for other values of δ were also found to be in good agreement with experimental results.
Therefore, characteristics of the tested type of jet pump can be predicted to a high degree of accuracy by means of the expression

$$\pi = \frac{(1+K_s) - (1+K_t)\mu^2 \dfrac{\delta^4}{(1-\delta^2)^2}}{2\delta^2 + 2\mu^2 \dfrac{\delta^4}{1-\delta^2} - (1+K_t)\mu^2 \dfrac{\delta^4}{(1-\delta^2)^2} - (1+K_m+K_d)(1+\mu)^2\delta^4} ,$$

where

$$K_s = 0.05, \quad K_t = 0.05, \quad K_m = 0.06 \quad \text{and} \quad K_d = 0.14 .$$

In figure 17 theoretical characteristics are given for nine different values of the diameter ratio δ, namely, 0.2, 0.25, 0.3, 0.4, 0.5, 0.6, 0.7, 0.8 and 0.9.

For each of these δ values the relationship between the jet pump efficiency η and the mass flow ratio μ could also be calculated since η is defined by

$$\eta = \frac{\mu}{\pi - 1} \quad .$$

The results are shown in figure 18; it is seen from this figure that the maximum efficiency is dependent upon the value of the diameter ratio δ.

In figure 19 the maximum jet pump efficiency η_m is given as a function of δ.

The mass flow ratio at maximum efficiency (μ_m) as a function of the diameter ratio δ is shown in figure 20; the total pressure ratio at maximum efficiency (π_m) as a function of δ is also shown.

It is evident from the figures 18 and 19 that the maximum efficiency is as high as 0.374 for a δ value of about 0.53; the maximum efficiency is in excess of 0.30 in the range between the δ values of 0.27 and 0.77.

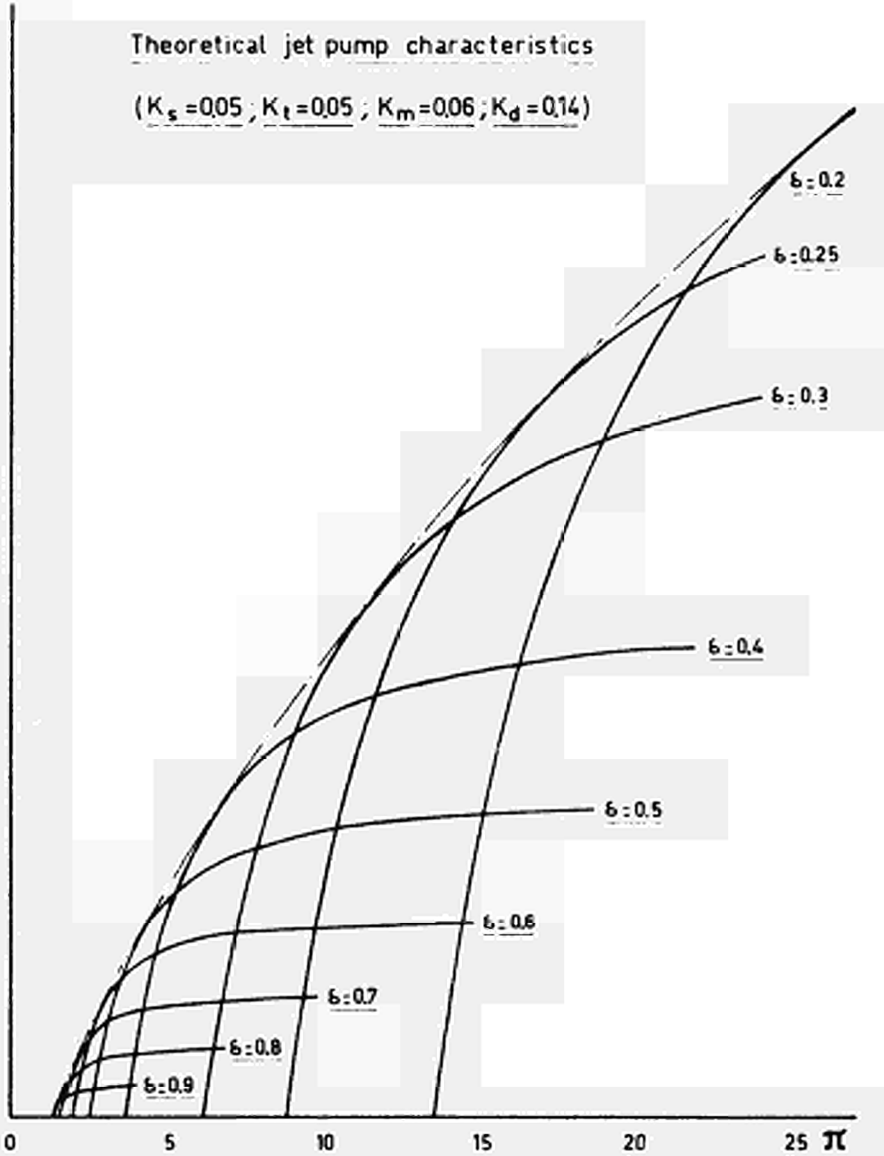

FIGURE 17

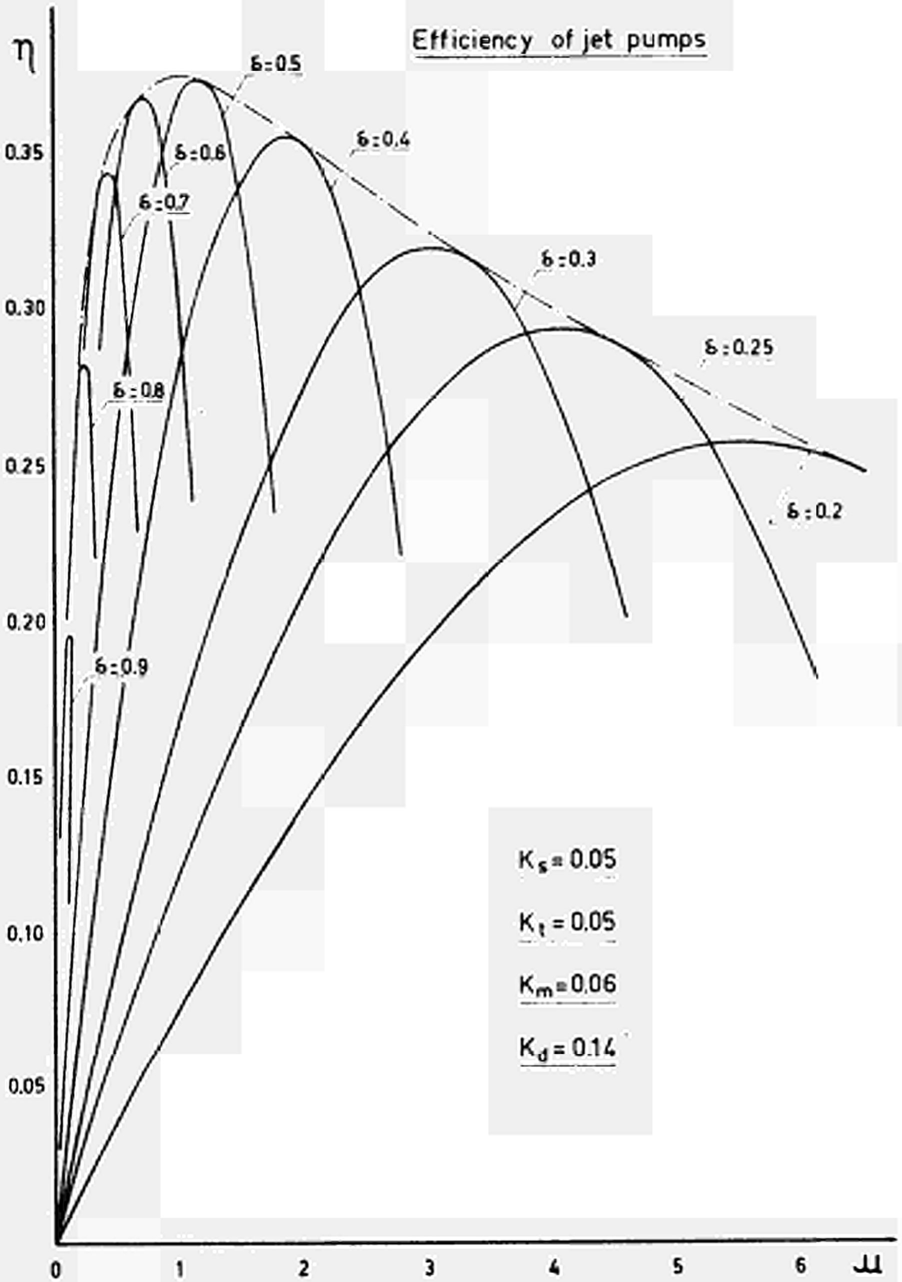

FIGURE 18

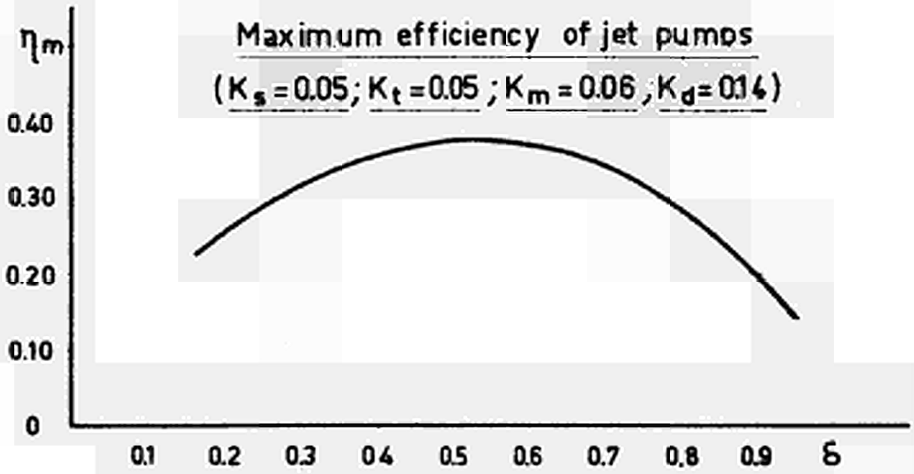

FIGURE 19

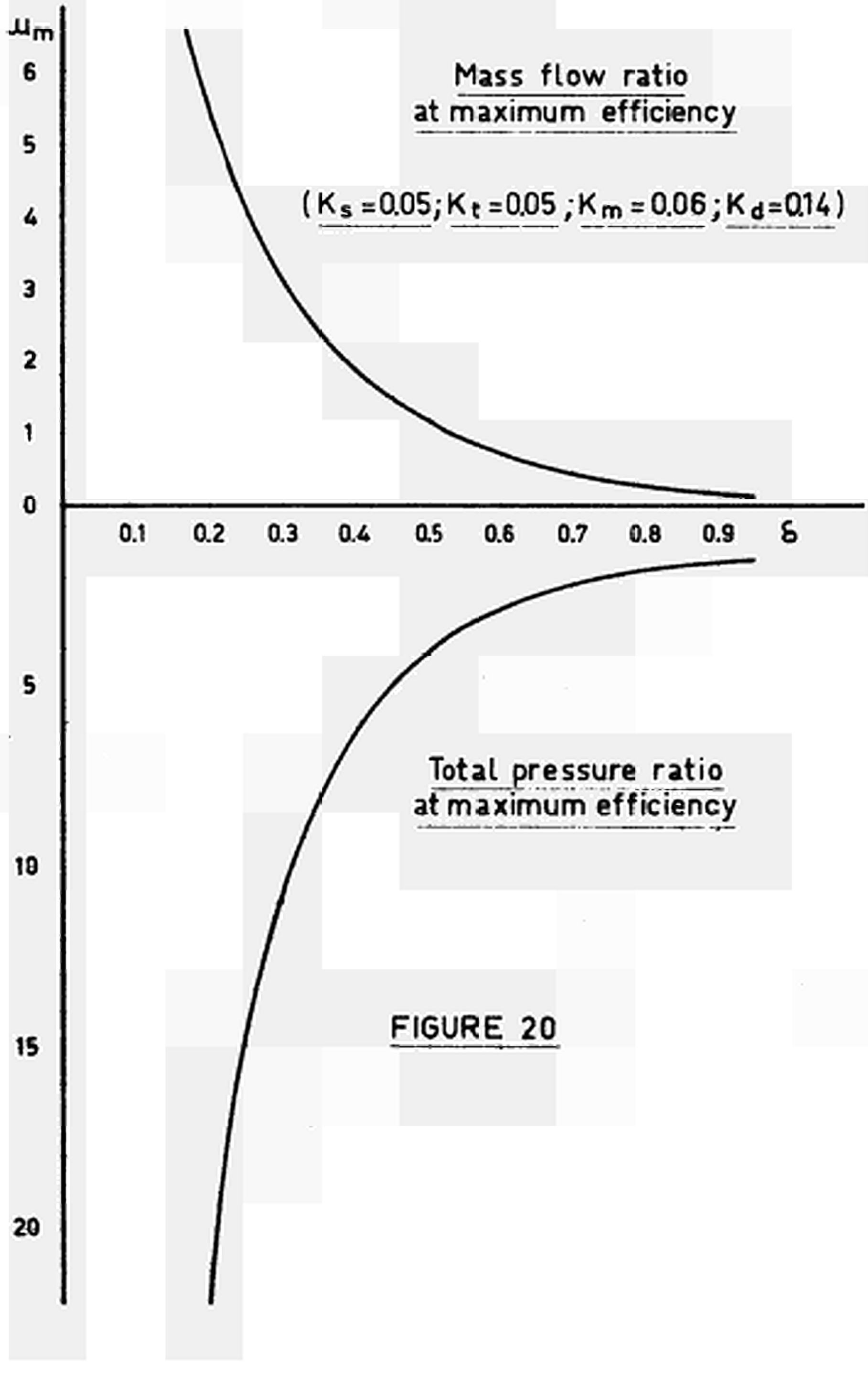

FIGURE 20

K. DETERMINATION OF ABSOLUTE DIMENSIONS

It was seen that in a steady state

$$H_A - H_B = \tfrac{1}{2}\rho v_s^2 \left\{ (1 + K_s) - (1 + K_t)\mu^2 \frac{\delta^4}{(1 - \delta^2)^2} \right\}$$

or

$$H_A - H_B = \varphi . \tfrac{1}{2}\rho v_s^2 \quad ,$$

where

$$\varphi = (1 + K_s) - (1 + K_t)\mu^2 \frac{\delta^4}{(1 - \delta^2)^2} \quad .$$

Since the total pressure ratio π is defined by

$$\pi = \frac{H_A - H_B}{H_C - H_B} \quad ,$$

it follows that

$$\pi(H_C - H_B) = \varphi . \tfrac{1}{2}\rho v_s^2$$

or

$$v_s = \sqrt{\frac{2\,\pi(H_C - H_B)}{\rho\varphi}} \quad .$$

From

$$S_s v_s = \frac{G_1}{\rho} \qquad \text{and} \qquad S_s = \frac{3.14}{4} d_s^2$$

it can be readily found that

$$d_s = \sqrt{\frac{4G_1}{3.14\rho v_s}} \quad .$$

Upon inserting the derived expression for v_s, the result is

$$d_s = 1.13\sqrt{G_1}\sqrt[4]{\frac{\varphi}{2\rho\pi(H_C - H_B)}} .$$

If in a system (figure 4), at maximum jet pump efficiency, the required values of the mass flow rates are G_1 and G_2, then the value of the mass flow ratio is

$$\mu_m = \frac{G_2}{G_1} .$$

The value of the diameter ratio δ for maximum jet pump efficiency at the required value of the mass flow ratio μ_m can be found from figure 20; for those values of μ_m and δ the value of the total pressure ratio Π_m can also be found.

For this case the value of the coefficient φ is

$$\varphi = (1 + K_s) - (1 + K_t)\mu_m^2 \frac{\delta^4}{(1 - \delta^2)^2} .$$

The difference in total pressure at C and B (figure 4) is equal to the sum of the separate pressure losses due to friction and to changes in velocity resulting from gradual or abrupt changes in the cross-sectional area of the fluid conduit CDB; hence the pressure loss $H_C - H_B$ at the required flow rates can be predicted from the surface roughness and the shape and size of the fluid passages of the conduit CDB.

Since δ is defined by

$$\delta = \frac{d_s}{d_m} ,$$

it follows that

$$d_m = \frac{d_s}{\delta} .$$

Other dimensions can be determined from d_s and d_m since for the considered type of jet pump (figure 5)

$$l_n = 6\ d_s\ ,\quad l_e = 0.7\ d_m\ ,\quad l_m = 8\ d_m\ ,\quad l_d = 10\ d_m\ ,$$

$$r = 0.5\ d_m\ , \alpha = 10^\circ - 15^\circ\ ,\quad \beta = 7^\circ .$$

Example

If it is required that, at maximum jet pump efficiency, the mass flow rates G_1 and G_2 are 12.2 kg/sec and 19.7 kg/sec, respectively, then the required mass flow ratio μ_m is

$$\mu_m = \frac{G_2}{G_1} = \frac{19.7}{12.2} = 1.61 \quad .$$

It is seen from figure 20 that for the μ_m value of 1.61 the diameter ratio δ is 0.43; for these values of μ_m and δ the value of the total pressure ratio π_m is seen to be about 5.5.

For μ_m = 1.61 the coefficient φ is, if $K_s = K_t = 0.05$,

$$\varphi = (1 + K_s) - (1 + K_t)\mu_m^2 \frac{\delta^4}{(1 - \delta^2)^2} =$$

$$= 1.05 - 1.05 \times 1.61^2 \frac{0.43^4}{(1 - 0.43^2)^2} = 0.91 \quad .$$

If the fluid density is taken as 750 kg/m^3 and the pressure loss $H_C - H_B$ as 50 000 N/m^2, it follows that the diameter of the nozzle tip is

$$d_s = 1.13\sqrt{G_1}\sqrt[4]{\frac{\varphi}{2\rho\pi_m(H_C - H_B)}} =$$

$$= 1.13\sqrt{12.2}\sqrt[4]{\frac{0.91}{2 \times 750 \times 5.5 \times 50000}} = 0.0271 \text{ m} =$$

$$= 27.1 \text{ mm} \quad .$$

The diameter of the mixing tube is

$$d_m = \frac{d_s}{\delta} = \frac{27.1}{0.43} = 63.0 \text{ mm} \quad .$$

For the considered type of jet pump (figure 5)

$l_n = 6\ d_s$, $l_e = 0.7\ d_m$, $l_m = 8\ d_m$, $l_d = 10\ d_m$,

$r = 0.5\ d_m$, $\alpha = 10^\circ - 15^\circ$, $\beta = 7^\circ$.

It follows, therefore, that

$l_n = 163$ mm , $l_e = 44$ mm , $l_m = 504$ mm , $l_d = 630$ mm

$r = 31$ mm .

L. CONCLUSIONS

a. The performance of a jet pump is dependent upon the shape of the jet pump characteristic.

b. The characteristic of a jet pump with a given diameter ratio δ can be predicted by means of the equation

$$\pi = \frac{(1+K_s)-(1+K_t)\mu^2\dfrac{\delta^4}{(1-\delta^2)^2}}{2\delta^2+2\mu^2\dfrac{\delta^4}{1-\delta^2}-(1+K_t)\mu^2\dfrac{\delta^4}{(1-\delta^2)^2}-(1+K_m+K_d)(1+\mu)^2\delta^4};$$

good agreement with experimentally found characteristics of high-performance jet pumps was obtained for

$$K_s = 0.05\ ,\quad K_t = 0.05\ ,\quad K_m = 0.06 \quad\text{and}\quad K_d = 0.14.$$

c. High jet pump performance was attained when the following conditions were satisfied (figure 5):

$$\begin{aligned} l_n &= 6\ d_s \\ \alpha &= 10^\circ\text{–}15^\circ \\ e &< 0.16 \\ r &= 0.5\ d_m \\ l_e &= 0.7\ d_m \\ l_m &= 8\ d_m \\ l_d &= 10\ d_m \\ \beta &= 7^\circ\ . \end{aligned}$$

Internal surfaces: Smooth (normally polished).

d. For a given type of jet pump the maximum efficiency is dependent upon the value of the diameter ratio.

e. An efficiency in excess of 0.37 can be realized.

ACKNOWLEDGEMENT

The author wishes to acknowledge the cooperation of E. Buur, who assisted in constructing and operating the experimental equipment, and L. van Zijl, who prepared the figures.

REFERENCES

G. Flügel, "Berechnung von Strahlapparaten", VDI-Forschungsheft 395; Deutscher Ingenieur-Verlag, Düsseldorf.

F. Schulz and K.H. Fasol, "Wasserstrahlpumpen zur Förderung von Flüssigkeiten"; Wien, Springer-Verlag, 1958.

"VDI-Durchflussmessregeln"; Deutscher Ingenieur-Verlag, Düsseldorf.

APPENDIX

1. Reduction of the test data

1.1. Pressure losses

The difference in total pressure at two points (the pressure loss between two points) can be determined by means of a U-tube manometer.

If a U-tube manometer is connected to static pressure taps located at X and D (figure 5), then

$$p_X + \rho g(h_X - h_D) + \rho g E_{XD} = p_D + \rho_m g E_{XD} \quad ,$$

where

- p_X is the static pressure at X,
- p_D is the static pressure at D,
- ρ is the density of the fluid,
- ρ_m is the density of the manometer fluid,
- g is the acceleration due to gravity,
- h_X is the height of X above the reference level 0-0,
- h_D is the height of D above the reference level 0-0,
- E_{XD} is the manometer deflection.

Hence

$$p_X - p_D + \rho g(h_X - h_D) = (\rho_m - \rho) g E_{XD} \quad .$$

If v_X and v_D are the fluid velocities at X and D, respectively, the total pressure H_X at X is

$$H_X = p_X + \rho g h_X + \tfrac{1}{2}\rho v_X^2$$

and the total pressure H_D at D is

$$H_D = p_D + \rho g h_D + \tfrac{1}{2}\rho v_D^2 \quad .$$

Therefore, the pressure loss between X and D is

$$H_X - H_D = p_X - p_D + \rho g(h_X - h_D) + \tfrac{1}{2}\rho(v_X^2 - v_D^2) =$$

$$= (\rho_m - \rho)gE_{XD} + \tfrac{1}{2}\rho(v_X^2 - v_D^2) \quad .$$

The difference in total pressure at two points (the pressure loss between two points) can also be calculated from the readings of two separate pressure gauges.

If a pressure gauge M_A is connected to a pressure tap located at A and a pressure gauge M_D is connected to a pressure tap located at D (figure 5), then

$$E_A - E_D = p_A + \rho g(h_A - h_{MA}) - \left\{ p_D + \rho g(h_D - h_{MD})\right\},$$

where

- E_A is the reading of the pressure gauge M_A,
- E_D is the reading of the pressure gauge M_D,
- p_A is the static pressure at A,
- h_A is the height of A above the reference level 0-0,
- h_{MA} is the height of the pressure gauge M_A above the reference level 0-0,
- h_{MD} is the height of the pressure gauge M_D above the reference level 0-0.

Hence

$$p_A - p_D + \rho g(h_A - h_D) = E_A - E_D + \rho g(h_{MA} - h_{MD}) .$$

If

v_A is the fluid velocity at A,

H_A is the total pressure at A,

H_D is the total pressure at D,

then the pressure loss between A and D is

$$H_A - H_D = p_A - p_D + \rho g(h_A - h_D) + \tfrac{1}{2}\rho(v_A^2 - v_D^2) =$$

$$= E_A - E_D + \rho g(h_{MA} - h_{MD}) + \tfrac{1}{2}\rho(v_A^2 - v_D^2).$$

1.2. Mass flow rates

Orifice plates O_1 and O_2 (figure 3) were used to determine the mass flow rates G_1 and $G_1 + G_2$, respectively (figures 1 and 4).

If

Δp_1 is the static pressure drop across the orifice plate O_1,

Δp_2 is the static pressure drop across the orifice plate O_2,

then the mass flow rates G_1 and $G_1 + G_2$ are given by

$$G_1 = \alpha_{01} \cdot \frac{\pi}{4} d_{01}^2 \sqrt{2 \rho \Delta p_1} \quad ,$$

$$G_1 + G_2 = \alpha_{02} \cdot \frac{\pi}{4} d_{02}^2 \sqrt{2 \rho \Delta p_2} \quad ,$$

where

α_{01} and α_{02} are flow coefficients for the orifice plates O_1 and O_2, respectively,

d_{01} and d_{02} are the diameters of the orifices in the plates O_1 and O_2, respectively.

If U-tube manometers are used to determine the static pressure differences across the orifice plates O_1 and O_2, then

$$\Delta p_1 = (\rho_m - \rho) g E_{01} \quad ,$$

$$\Delta p_2 = (\rho_m - \rho) g E_{02} \quad ,$$

where E_{01} and E_{02} are the manometer deflections for the orifice plates O_1 and O_2, respectively.

Hence

$$G_1 = \alpha_{01} \cdot \frac{\pi}{4}\, d_{01}^2 \sqrt{2\rho(\rho_m - \rho)g} \sqrt{E_{01}} \,,$$

$$G_1 + G_2 = \alpha_{02} \cdot \frac{\pi}{4}\, d_{02}^2 \sqrt{2\rho(\rho_m - \rho)g} \sqrt{E_{02}} \,.$$

1.3. The mass flow ratio

The mass flow ratio μ is defined by

$$\mu = \frac{G_2}{G_1} \quad .$$

It was already found that

$$G_1 + G_2 = \alpha_{02} \cdot \frac{\pi}{4} d_{02}^2 \sqrt{2\rho(\rho_m - \rho)g} \sqrt{E_{02}} \quad ,$$

$$G_1 = \alpha_{01} \cdot \frac{\pi}{4} d_{01}^2 \sqrt{2\rho(\rho_m - \rho)g} \sqrt{E_{01}} \quad .$$

Hence

$$\mu = \frac{G_2}{G_1} = \frac{G_1 + G_2}{G_1} - 1 =$$

$$= \frac{\alpha_{02} \cdot \frac{\pi}{4} d_{02}^2 \sqrt{2\rho(\rho_m - \rho)g} \sqrt{E_{02}}}{\alpha_{01} \cdot \frac{\pi}{4} d_{01}^2 \sqrt{2\rho(\rho_m - \rho)g} \sqrt{E_{01}}} - 1$$

or

$$\mu = \frac{\alpha_{02} \cdot d_{02}^2}{\alpha_{01} \cdot d_{01}^2} \sqrt{\frac{E_{02}}{E_{01}}} - 1 \quad .$$

1.4. Velocities

The fluid velocity v_s in the discharge tip of the driving nozzle (figures 1 and 5) is

$$v_s = \frac{G_1}{\rho S_s} = \frac{S_m}{S_s}\frac{G_1}{\rho S_m} = \left(\frac{d_m}{d_s}\right)^2 \frac{G_1}{\rho S_m} = \frac{1}{\delta^2}\frac{G_1}{\rho S_m} \quad ,$$

where

G_1 is the mass flow rate in the driving nozzle,

d_s and d_m are the diameters of the nozzle tip and the mixing tube, respectively,

S_s and S_m are the flow areas of the nozzle tip and the mixing tube, respectively,

δ is the diameter ratio, defined by

$$\delta = \frac{d_s}{d_m} \quad .$$

It was already found that

$$G_1 = \alpha_{01} \cdot \frac{\pi}{4} d_{01}^2 \sqrt{2\rho(\rho_m - \rho)g}\sqrt{E_{01}} \quad ;$$

it follows, therefore, that

$$v_s = \frac{1}{\delta^2 S_m}\left\{\alpha_{01} \cdot \frac{\pi}{4} d_{01}^2 \sqrt{2(\rho_m - \rho)g}\right\}\frac{1}{\sqrt{\rho}}\sqrt{E_{01}} \quad .$$

The velocity v_Z at the outlet end of the mixing tube (figure 5) is

$$v_Z = \frac{G_1 + G_2}{\rho S_m} \quad ,$$

where G_2 is the mass flow rate in the suction section of the jet pump.

Hence

$$v_Z = (1 + \mu) \frac{G_1}{\rho S_m} \quad ,$$

where μ is the mass flow ratio, defined by

$$\mu = \frac{G_2}{G_1} \quad .$$

If

S_A is the cross-sectional area upstream from the driving nozzle at A,

S_B is the flow area in the suction section at B,

S_C is the flow area at the diffuser outlet at C,

then

$$v_A = \frac{G_1}{\rho S_A} = \frac{G_1}{\rho S_m} \frac{S_m}{S_A} \quad ,$$

$$v_B = \frac{G_2}{\rho S_B} = \frac{\mu G_1}{\rho S_B} = \mu \frac{G_1}{\rho S_m} \frac{S_m}{S_B} \quad ,$$

$$v_C = \frac{G_1 + G_2}{\rho S_C} = \frac{(1 + \mu) G_1}{\rho S_C} = (1 + \mu) \frac{G_1}{\rho S_m} \frac{S_m}{S_C} \quad .$$

Consequently, since $\dfrac{G_1}{\rho S_m} = \delta^2 v_s$,

$$v_Z = (1 + \mu) \delta^2 v_s \quad , \qquad v_A = \frac{S_m}{S_A} \delta^2 v_s \quad ,$$

$$v_B = \frac{S_m}{S_B} \mu \delta^2 v_s \quad , \qquad v_C = \frac{S_m}{S_C} (1 + \mu) \delta^2 v_s \; .$$

1.5. The total pressure ratio

The total pressure ratio π is defined by

$$\pi = \frac{H_A - H_B}{H_C - H_B} \quad ,$$

where (figures 1 and 5)

H_A is the total pressure in the plane A,

H_B is the total pressure in the plane B,

H_C is the total pressure in the plane C.

The ratio π may also be written as

$$\pi = \frac{(H_A - H_D) - (H_B - H_D)}{(H_C - H_D) - (H_B - H_D)} \quad ,$$

where H_D is the total pressure at D.

To determine the difference in total pressure at A and D separate spring-type gauges M_A and M_D were used (figures 3 and 5).

The difference in total pressure at C and D and the difference in total pressure at B and D were determined by means of U-tube manometers (figure 3).

Hence

$$\pi = \frac{(H_A - H_D) - (H_B - H_D)}{(H_C - H_D) - (H_B - H_D)} =$$

$$= \frac{\left\{E_A - E_D + \rho g(h_{MA} - h_{MD}) + \frac{1}{2}\rho(v_A^2 - v_D^2)\right\} - \left\{(\rho_m - \rho) g E_{BD} + \frac{1}{2}\rho(v_B^2 - v_D^2)\right\}}{\left\{(\rho_m - \rho) g E_{CD} + \frac{1}{2}\rho(v_C^2 - v_D^2)\right\} - \left\{(\rho_m - \rho) g E_{BD} + \frac{1}{2}\rho(v_B^2 - v_D^2)\right\}} =$$

$$= \frac{E_A - E_D + \rho g(h_{MA} - h_{MD}) - (\rho_m - \rho) g E_{BD} + \frac{1}{2}\rho(v_A^2 - v_B^2)}{(\rho_m - \rho) g (E_{CD} - E_{BD}) + \frac{1}{2}\rho(v_C^2 - v_B^2)} \quad ,$$

where

E_A and E_D are the readings of the pressure gauges M_A and M_D, respectively,

E_{BD} is the deflection of the U-tube manometer which is connected to pressure taps located at B and D,

E_{CD} is the deflection of the U-tube manometer which is connected to pressure taps located at C and D,

h_{MA} is the height of the pressure gauge M_A above the reference level 0-0,

h_{MD} is the height of the pressure gauge M_D above the reference level 0-0,

v_A is the fluid velocity at A,

v_B is the fluid velocity at B,

v_C is the fluid velocity at C,

v_D is the fluid velocity at D.

Consequently, the values of the total pressure ratio π can be calculated from the readings E_{01}, E_{02}, E_A, E_D, E_{BD} and E_{CD} by means of the following equations:

$$\mu = \frac{\alpha_{02} \cdot d_{02}^2}{\alpha_{01} \cdot d_{01}^2} \sqrt{\frac{E_{02}}{E_{01}}} - 1 \quad ,$$

$$v_s = \frac{1}{\delta^2 S_m} \left\{ \alpha_{01} \cdot \frac{\pi}{4} d_{01}^2 \sqrt{2(\rho_m - \rho) g} \right\} \frac{1}{\sqrt{\rho}} \sqrt{E_{01}} \quad ,$$

$$v_A = \frac{S_m}{S_A} \delta^2 v_s \quad ,$$

$$v_B = \frac{S_m}{S_B} \mu \delta^2 v_s \quad ,$$

$$v_C = \frac{S_m}{S_C} (1 + \mu) \delta^2 v_s \quad ,$$

$$\pi = \frac{E_A - E_D + \rho g (h_{MA} - h_{MD}) - (\rho_m - \rho) g E_{BD} + \frac{1}{2}\rho (v_A^2 - v_B^2)}{(\rho_m - \rho) g (E_{CD} - E_{BD}) + \frac{1}{2}\rho (v_C^2 - v_B^2)} \quad .$$

1.6. Significant data

a. Orifice plates (figure 3)

Flow coefficient for orifice plate O_1	: $\alpha_{01} = 0.656$
Flow coefficient for orifice plate O_2	: $\alpha_{02} = 0.649$
Diameter of orifice in plate O_1	: $d_{01} = 48.95 \times 10^{-3}$ m
Diameter of orifice in plate O_2	: $d_{02} = 83.26 \times 10^{-3}$ m

b. U-tube manometers (figure 3)

Density of manometer fluid (mercury)	: $\rho_m = 13600$ kg/m^3
(Acceleration due to gravity:	$g = 9.81$ m/sec^2)

c. Jet pump (figures 1, 3 and 5)

Diameter of mixing tube	: $d_m = 60.1 \times 10^{-3}$ m
Flow area at Z	: $S_Z = 28.4 \times 10^{-4}$ m^2
Flow area at A	: $S_A = 19.6 \times 10^{-4}$ m^2
Flow area at B	: $S_B = 112 \times 10^{-4}$ m^2
Flow area at C	: $S_C = 140 \times 10^{-4}$ m^2

d. Pressure gauges (figures 3 and 5)

Vertical distance between pressure gauges M_A and M_D	: $h_{MA} - h_{MD} = 0.9$ m

2. Tables 2 to 13

PHASE II	t °C	E_{01} cm Hg	E_{02} cm Hg	$E_A - E_D$ N/m^2	E_{CD} cm Hg	E_{BD} cm Hg	v_s m/sec	μ	π	FIGURE
	25	35.8	4.4	199072	60.6	0	21.4	0.01	2.99	
	25	35.8	5.5	199206	58.3	0	21.4	0.12	3.10	
δ = 0.439	25	35.8	7.9	199520	54.9	- 0.4	21.4	0.35	3.29	
e = 0.16	25	35.9	9.9	199606	51.4	- 0.9	21.4	0.51	3.47	
r = 5 d_m	25	34.7	12.7	189262	43.2	- 2.1	21.1	0.74	3.85	6
l_e = 0.7 d_m	25	34.9	16.7	191224	38.7	- 3.1	21.1	0.98	4.22	
l_m = 8 d_m	25	36.7	20.8	193273	35.5	- 4.5	21.7	1.16	4.50	
l_d = 10 d_m	25	37.4	27.9	187967	24.6	- 7.3	21.8	1.48	5.60	

TABLE 2

PHASE III	t °C	E_{01} cm Hg	E_{02} cm Hg	$E_A - E_D$ N/m^2	E_{CD} cm Hg	E_{BD} cm Hg	v_s m/sec	μ	π	FIGURE
	25	8.1	1.1	147079	25.6	0	16.8	0.05	5.03	
	25	8.1	1.6	147079	24.7	0	16.8	0.27	5.21	
	25	8.2	2.9	146098	22.5	- 0.4	16.9	0.71	5.60	
	25	8.2	4.3	145117	20.7	- 0.9	16.9	1.08	5.93	—
	25	8.3	5.8	145117	18.6	- 1.6	17.1	1.39	6.37	
	25	8.3	7.1	145117	16.8	- 2.2	17.1	1.66	6.80	
	25	8.5	9.0	143155	14.5	- 3.2	17.3	1.96	7.27	
	25	8.6	11.2	142174	11.6	- 4.2	17.4	2.26	8.16	
δ = 0.339	25	15.3	1.9	278800	48.3	0	23.2	0.01	4.94	
e = 0.16	25	15.3	3.2	277819	45.7	- 0.1	23.2	0.31	5.17	
r = 5 d_m	25	15.3	5.4	278086	42.5	- 0.5	23.2	0.71	5.51	
l_e = 0.7 d_m	25	15.4	7.9	277105	39.4	- 1.2	23.2	1.06	5.85	—
l_m = 8 d_m	25	15.5	9.4	276391	37.5	- 1.7	23.3	1.23	6.06	
l_d = 10 d_m	25	15.8	14.5	274696	31.8	- 3.5	23.5	1.74	6.73	
	25	16.0	18.9	274386	26.7	- 5.2	23.7	2.12	7.47	
	25	16.1	22.9	272286	22.4	- 6.8	23.8	2.42	8.16	
	25	20.0	2.9	358975	61.9	0	26.4	0.09	4.91	
	25	20.0	5.0	357013	58.3	- 0.4	26.4	0.44	5.19	
	25	20.0	6.5	357013	56.2	- 0.7	26.4	0.64	5.35	
	25	20.1	11.2	351127	50.2	- 2.3	26.5	1.14	5.71	—
	25	20.4	14.9	351127	45.3	- 4.8	26.7	1.45	6.04	
	25	20.[illegible]	20.3	3[illegible]11[illegible]7	39.2	- 6.1	26.6	1.85	6.70	
	25	20.8	25.8	351127	32.0	- 8.7	27.0	2.20	7.52	
	25	21.0	29.9	351127	26.8	-10.9	27.1	2.45	8.17	

TABLE 3

PHASE IV	t °C	E_{01} cm Hg	E_{02} cm Hg	$E_A - E_D$ N/m^2	E_{CD} cm Hg	E_{BD} cm Hg	v_s m/sec	μ	π	FIGURE
	25	20.2	2.5	111230	34.1	0	16.1	0.01	3.02	10
	25	20.2	3.3	111230	32.6	0	16.1	0.16	3.16	
	25	20.2	4.1	111230	31.2	- 0.1	16.1	0.29	3.29	
	25	20.2	5.1	111230	29.6	- 0.3	16.1	0.44	3.48	
	25	20.2	6.7	110249	27.0	- 0.8	16.1	0.65	3.69	
	25	20.4	8.3	110249	24.4	- 1.2	16.2	0.83	4.03	
	25	20.8	10.3	108518	21.6	- 1.9	16.3	1.02	4.42	
	25	21.0	12.7	108518	17.5	- 2.7	16.4	1.23	5.19	
δ = 0.439	25	21.2	14.7	103613	13.5	- 3.5	16.5	1.39	5.95	
e = 0.16	25	34.2	4.9	189441	55.8	0	20.9	0.08	3.09	6,10
r = 5 d_m	25	34.2	6.0	191403	54.5	- 0.1	20.9	0.20	3.19	
l_e = 0.7 d_m	25	34.2	7.5	190422	52.1	- 0.3	20.9	0.34	3.32	
l_m = 8 d_m	25	34.3	9.3	189441	49.0	- 0.8	21.0	0.49	3.48	
l_d = 10 d_m	25	34.4	11.7	187479	45.2	- 1.4	21.0	0.67	3.70	
	25	34.6	13.7	186498	42.4	- 2.0	21.0	0.80	3.84	
	25	34.8	16.0	185654	38.6	- 2.6	21.1	0.95	4.17	
	25	35.1	20.1	181730	31.7	- 4.0	21.2	1.18	4.76	
	25	35.4	25.1	177090	22.8	- 6.0	21.2	1.41	5.81	
	25	43.2	6.0	238491	70.4	- 0.1	23.6	0.06	3.05	10
	25	43.0	10.4	237510	63.4	- 0.7	23.5	0.41	3.35	
	25	43.3	15.7	235548	55.5	- 2.0	23.6	0.73	3.73	
	25	43.7	19.7	232605	49.0	- 3.2	23.7	0.92	4.09	
	25	44.2	25.9	225875	38.3	- 5.4	23.8	1.20	4.80	
	25	44.7	33.6	220833	28.7	- 7.7	23.9	1.48	5.71	

TABLE 4

PHASE V	t °C	E_{01} cm Hg	E_{02} cm Hg	$E_A - E_D$ N/m^2	E_{CD} cm Hg	E_{BD} cm Hg	v_s m/sec	μ	π	FIGURE
	25	14.2	1.8	258513	44.9	0	22.3	0.02	4.95	—
	25	14.2	2.6	255570	42.4	- 0.1	22.3	0.23	5.19	
	25	14.3	5.1	260930	39.4	- 0.5	22.4	0.71	5.54	
	25	14.5	8.8	257218	34.7	- 1.7	22.6	1.23	6.12	
δ = 0.339	25	14.5	11.0	257748	32.0	- 2.5	22.6	1.50	6.49	
e = 0.16	25	14.7	14.3	257042	27.8	- 3.7	22.7	1.83	7.07	
r = 5 d_m	25	14.9	17.5	256061	23.1	- 5.0	22.9	2.11	7.93	
	25	15.0	20.3	256453	19.2	- 6.1	22.9	2.34	8.85	
l_e = 0.7 d_m	25	21.6	2.8	387603	67.6	0	27.5	0.03	4.87	—
l_m = 8 d_m	25	21.5	5.1	387868	63.1	- 0.1	27.5	0.39	5.20	
l_d = 10 d_m	25	21.6	8.0	387868	59.2	- 1.0	27.5	0.74	5.47	
	25	21.8	11.9	388142	54.2	- 2.2	27.6	1.12	5.86	
	25	22.0	16.3	396255	48.7	- 3.6	27.7	1.47	6.32	
	25	22.2	22.6	379264	40.4	- 6.0	27.8	1.90	7.03	
	25	22.4	26.5	379529	34.7	- 7.7	28.0	2.13	7.73	
	25	22.5	30.4	379529	29.3	- 9.4	28.1	2.34	8.51	

TABLE 5

PHASE VI	t (°C)	E_{01} (cm Hg)	E_{02} (cm Hg)	$E_A - E_D$ (N/m^2)	E_{CD} (cm Hg)	E_{BD} (cm Hg)	v_s (m/sec)	μ	π	FIGURE
$\delta = 0.403$ $e = 0.16$ $r = 5\ d_m$ $l_c = 0.7\ d_m$ $l_m = 8\ d_m$ $l_d = 10\ d_m$	25	22.8	3.0	194167	47.8	0	20.1	0.04	3.66	7
	25	22.8	3.4	196129	46.5	0	20.1	0.11	3.77	
	25	22.8	4.8	196129	44.9	- 0.2	20.1	0.32	3.86	
	25	23.0	7.0	194167	41.5	- 0.6	20.2	0.58	4.10	
	25	23.1	10.0	192472	37.2	- 1.5	20.2	0.89	4.45	
	25	23.4	13.6	190510	32.4	- 2.5	20.4	1.20	4.91	
	25	23.7	17.2	187567	26.9	- 3.9	20.5	1.45	5.54	
	25	23.9	21.7	184665	20.0	- 5.6	20.6	1.74	6.62	

TABLE 6

PHASE VII	t (°C)	E_{01} (cm Hg)	E_{02} (cm Hg)	$E_A - E_D$ (N/m^2)	E_{CD} (cm Hg)	E_{BD} (cm Hg)	v_s (m/sec)	μ	π	FIGURE
$\delta = 0.403$ $e = 0.16$ $r = 0.5\ d_m$ $l_e = 0.7\ d_m$ $l_m = 8\ d_m$ $l_d = 10\ d_m$	25	23.3	3.1	202149	49.6	0	20.3	0.05	3.61	7,8
	25	23.4	4.3	201168	47.0	0	20.3	0.23	3.79	
	25	23.4	6.7	200187	43.3	- 0.6	20.3	0.53	4.04	
	25	23.6	9.7	200187	38.9	- 1.4	20.4	0.84	4.42	
	25	23.7	12.7	199206	35.0	- 2.4	20.5	1.10	4.77	
	25	23.7	16.1	199206	30.5	- 3.8	20.5	1.36	5.24	
	25	23.8	19.3	197244	25.6	- 5.3	20.6	1.62	5.81	
	25	23.9	23.4	196263	20.8	- 6.8	20.6	1.84	6.52	

TABLE 7

PHASE VIII	t °C	E_{01} cm Hg	E_{02} cm Hg	$E_A - E_D$ N/m^2	E_{CD} cm Hg	E_{BD} cm Hg	v_s m/sec	μ	π	FIGURE
	25	20.5	2.8	113992	34.5	0	16.2	0.06	3.08	11
	25	20.5	3.9	113992	32.1	0	16.2	0.25	3.31	
	25	20.5	5.3	113011	29.8	- 0.3	16.2	0.45	3.51	
	25	20.6	7.1	113278	27.2	- 0.7	16.2	0.68	3.80	
	25	20.7	9.1	112297	24.4	- 1.2	16.3	0.90	4.15	
	25	20.7	11.1	112564	21.6	- 1.8	16.3	1.10	4.56	
	25	20.9	13.5	110602	18.4	- 2.5	16.4	1.30	5.13	
$\delta = 0.439$	25	21.0	16.0	110602	15.0	- 3.1	16.4	1.50	5.86	
$e = 0.16$	25	34.7	5.1	193453	57.5	0	21.1	0.10	3.07	11
$r = 0.5\ d_m$	25	34.7	7.7	192472	52.5	- 0.4	21.1	0.35	3.33	
$l_e = 0.7\ d_m$	25	34.7	11.3	192472	47.0	- 1.0	21.1	0.64	3.68	
$l_m = 8\ d_m$	25	34.9	14.7	191758	42.5	- 1.8	21.1	0.85	3.96	
$l_d = 10\ d_m$	25	35.0	18.3	190062	37.3	- 2.8	21.2	1.08	4.41	
	25	35.2	22.4	189617	31.7	- 4.1	21.2	1.28	4.91	
	25	35.2	27.1	187871	25.3	- 5.7	21.2	1.52	5.67	
	25	44.3	8.6	243454	68.9	- 0.1	23.8	0.26	3.19	11,12
	25	44.3	12.7	243884	62.5	- 0.8	23.8	0.54	3.49	
	25	44.4	17.0	243884	56.4	- 1.8	23.8	0.77	3.81	
	25	44.4	22.0	240227	49.0	- 3.4	23.8	1.02	4.19	
	25	44.5	28.0	238667	40.6	- 5.3	23.8	1.28	4.79	
	25	44.7	34.1	237108	31.8	- 7.4	23.9	1.51	5.61	

TABLE 8

PHASE IX	t °C	E_{01} cm Hg	E_{02} cm Hg	$E_A - E_D$ N/m^2	E_{CD} cm Hg	E_{BD} cm Hg	v_s m/sec	μ	π	FIGURE
$\delta = 0.439$	57	44.3	8.5	239960	68.8	0	23.9	0.26	3.16	12
$e = 0.16$	57	44.3	12.7	239960	61.9	- 0.8	23.9	0.54	3.47	
$r = 0.5\ d_m$	57	44.5	17.0	239113	55.3	- 1.9	24.0	0.77	3.81	
$l_e = 0.7\ d_m$	57	44.5	21.9	237418	48.0	- 3.4	24.0	1.01	4.24	
$l_m = 8\ d_m$	57	44.7	28.0	234606	38.1	- 5.5	24.1	1.27	4.97	
$l_d = 10\ d_m$	57	44.7	32.8	230947	30.1	- 7.4	24.1	1.46	5.65	

TABLE 9

PHASE X	t °C	E_{01} cm Hg	E_{02} cm Hg	$E_A - E_D$ N/m²	E_{CD} cm Hg	E_{BD} cm Hg	v_s m/sec	μ	π	FIGURE
	25	25.1	3.4	217892	53.0	0	21.0	0.05	3.63	
	25	25.2	4.6	216911	50.9	- 0.1	21.0	0.23	3.75	
	25	25.2	5.8	216911	48.8	- 0.3	21.0	0.38	3.90	
	25	25.2	7.2	215930	46.4	- 0.6	21.0	0.53	4.06	
$\delta = 0.403$	25	25.2	8.6	215930	44.7	- 1.0	21.0	0.67	4.19	
$e = 0$	25	25.3	11.3	215930	40.9	- 1.8	21.1	0.92	4.50	
$r = 0.5\ d_m$	25	25.4	13.9	214948	37.7	- 2.8	21.2	1.12	4.75	8,9,13,16
$l_e = 0.7\ d_m$	25	25.5	15.8	214948	35.4	- 3.6	21.3	1.26	4.95	
$l_m = 8\ d_m$	25	25.6	18.8	212987	31.3	- 4.7	21.3	1.46	5.35	
$l_d = 10\ d_m$	25	25.6	21.6	212000	28.0	- 5.9	21.3	1.64	5.68	
	25	25.8	24.6	210891	25.0	- 7.1	21.4	1.80	6.01	
	25	25.8	26.2	210891	22.9	- 8.0	21.4	1.89	6.27	

TABLE 10

PHASE XI	t °C	E_{01} cm Hg	E_{02} cm Hg	$E_A - E_D$ N/m²	E_{CD} cm Hg	E_{BD} cm Hg	v_s m/sec	μ	π	FIGURE
	25	25.1	3.5	217625	53.1	0	21.0	0.07	3.64	
	25	25.1	4.6	217625	50.5	0	21.0	0.23	3.83	
	25	25.1	7.1	217625	46.2	- 0.6	21.0	0.53	4.12	
	25	25.2	9.9	216644	42.0	- 1.3	21.1	0.80	4.45	
$\delta = 0.403$	25	25.2	12.4	215796	38.3	- 2.1	21.1	1.01	4.77	
$e = 0.35$	25	25.3	14.0	215796	35.4	- 2.7	21.1	1.14	5.07	
$r = 0.5\ d_m$	25	25.4	15.8	214815	32.4	- 3.3	21.2	1.26	5.41	8
$l_e = 0.7\ d_m$	25	25.4	17.5	214815	29.9	- 3.9	21.2	1.38	5.72	
$l_m = 8\ d_m$	25	25.5	18.8	214815	27.1	- 4.8	21.2	1.46	6.09	
$l_d = 10\ d_m$	25	25.5	20.0	213854	25.2	- 5.2	21.2	1.54	6.38	
	25	25.6	21.6	212853	22.6	- 5.8	21.3	1.64	6.82	
	25	25.7	22.8	212720	20.6	- 7.0	21.3	1.70	7.06	

PHASE XII	t °C	E_{01} cm Hg	E_{02} cm Hg	$E_A - E_D$ N/m^2	E_{CD} cm Hg	E_{BD} cm Hg	v_s m/sec	μ	π	FIGURE
	25	25.0	3.5	217448	52.5	0	21.0	0.07	3.66	
	25	25.0	4.3	217448	51.0	0	21.0	0.19	3.77	
	25	25.1	5.6	216468	48.9	- 0.2	21.0	0.35	3.90	
	25	25.1	6.7	216468	47.2	- 0.6	21.0	0.48	4.01	
$\delta = 0.403$ $e = 0$ $r = 0.5\ d_m$ $l_e = 0.4\ d_m$ $l_m = 8\ d_m$ $l_d = 10\ d_m$	25	25.1	8.0	216468	45.4	- 0.8	21.0	0.62	4.15	
	25	25.3	9.8	214770	43.2	- 1.2	21.1	0.79	4.30	9
	25	25.3	12.0	213789	40.1	- 2.1	21.1	0.98	4.52	
	25	25.4	14.8	213789	36.6	- 3.0	21.1	1.19	4.84	
	25	25.4	17.4	209081	33.2	- 4.0	21.1	1.38	5.09	
	25	25.6	20.4	209149	29.4	- 5.2	21.2	1.56	5.48	
	25	25.6	23.6	207187	25.4	- 6.5	21.2	1.76	5.93	
	25	25.[illegible]	25.6	206206	23.4	- 7.4	21.4	1.86	6.14	

TABLE 12

PHASE XIII	t °C	E_{01} cm Hg	E_{02} cm Hg	$E_A - E_D$ N/m^2	E_{CD} cm Hg	E_{BD} cm Hg	v_s m/sec	μ	π	FIGURE
	25	16.5	3.0	295212	50.1	- 0.1	24.0	0.22	5.01	
	25	16.5	4.4	294231	47.5	- 0.3	24.0	0.48	5.25	
	25	16.5	6.1	294231	45.2	- 0.8	24.0	0.75	5.47	
$\delta = 0.339$ $e = 0$ $r = 0.5\ d_m$ $l_e = 0.7\ d_m$ $l_m = 8\ d_m$ $l_d = 10\ d_m$	25	16.5	7.6	294231	43.1	- 1.2	24.0	0.95	5.69	
	25	16.6	9.6	294496	40.7	- 2.0	24.1	1.18	5.92	
	25	16.7	11.6	294496	38.3	- 2.8	24.2	1.39	6.16	13,16
	25	16.7	13.6	294496	35.9	- 3.5	24.2	1.59	6.45	
	25	16.7	16.1	293515	33.2	- 4.6	24.2	1.82	6.72	
	25	16.9	19.9	293515	29.6	- 6.2	24.4	2.08	7.14	
	25	16.9	22.9	293515	25.9	- 7.8	24.4	2.34	7.63	
	25	16.9	25.4	293515	23.2	- 9.0	24.4	2.52	8.02	

TABLE 13

NOTICE TO THE READER

All Euratom reports are announced, as and when they are issued, in the monthly periodical **EURATOM INFORMATION,** edited by the Centre for Information and Documentation (CID). For subscription (1 year : US$ 15, £ 5.7) or free specimen copies please write to :

Handelsblatt GmbH
"Euratom Information"
Postfach 1102
D-4 Düsseldorf (Germany)

or

Office central de vente des publications
des Communautés européennes
2, Place de Metz
Luxembourg

To disseminate knowledge is to disseminate prosperity — I mean general prosperity and not individual riches — and with prosperity disappears the greater part of the evil which is our heritage from darker times.

Alfred Nobel

SALES OFFICES

All Euratom reports are on sale at the offices listed below, at the prices given on the back of the front cover (when ordering, specify clearly the EUR number and the title of the report, which are shown on the front cover).

OFFICE CENTRAL DE VENTE DES PUBLICATIONS
DES COMMUNAUTES EUROPEENNES
2, place de Metz, Luxembourg (Compte chèque postal Nº 191-90)

BELGIQUE — BELGIË
MONITEUR BELGE
40-42, rue de Louvain - Bruxelles
BELGISCH STAATSBLAD
Leuvenseweg 40-42, - Brussel

DEUTSCHLAND
BUNDESANZEIGER
Postfach - Köln 1

FRANCE
SERVICE DE VENTE EN FRANCE
DES PUBLICATIONS DES
COMMUNAUTES EUROPEENNES
26, rue Desaix - Paris 15e

ITALIA
LIBRERIA DELLO STATO
Piazza G. Verdi, 10 - Roma

LUXEMBOURG
OFFICE CENTRAL DE VENTE
DES PUBLICATIONS DES
COMMUNAUTES EUROPEENNES
9, rue Goethe - Luxembourg

NEDERLAND
STAATSDRUKKERIJ
Christoffel Plantijnstraat - Den Haag

UNITED KINGDOM
H. M. STATIONERY OFFICE
P. O. Box 569 - London S.E.1

EURATOM — C.I.D.
51-53, rue Belliard
Bruxelles (Belgique)